
AN EFFICIENT LOCAL SEARCH APPROACH FOR POLARIZED COMMUNITY DISCOVERY IN SIGNED NETWORKS

Linus Aronsson

Chalmers University of Technology
linaro@chalmers.se

Morteza Haghiri Chehreghani

Chalmers University of Technology
morteza.chehreghani@chalmers.se

ABSTRACT

Signed networks, where edges are labeled as positive or negative to indicate friendly or antagonistic interactions, offer a natural framework for studying polarization, trust, and conflict in social systems. Detecting meaningful group structures in these networks is crucial for understanding online discourse, political division, and trust dynamics. A key challenge is to identify groups that are cohesive internally yet antagonistic externally, while allowing for neutral or unaligned vertices. In this paper, we address this problem by identifying k polarized communities that are large, dense, and balanced in size. We develop an approach based on Frank-Wolfe optimization, leading to a local search procedure with provable convergence guarantees. Our method is both scalable and efficient, outperforming state-of-the-art baselines in solution quality while remaining competitive in terms of computational efficiency.

1 Introduction

Signed networks extend traditional graph representations by associating each edge with a positive or negative number, indicating friendly or antagonistic relationships. Originating from studies on social dynamics in the 1950s (Harary, 1953), signed networks introduce fundamental differences in graph structure that make many algorithms designed for unsigned networks inapplicable (Tang et al., 2016; Bonchi et al., 2019; Tzeng et al., 2020). These challenges have fueled extensive research in recent years, leading to advances in signed network embeddings, signed clustering, and signed link prediction. We refer to the survey by (Tang et al., 2016) for a comprehensive review of these methods. Most relevant to this paper is the problem of signed clustering, which we split into two categories: (i) *signed network partitioning* (SNP), and (ii) *polarized community discovery* (PCD). The latter is the problem studied in this paper.

The goal of signed clustering is to identify k conflicting groups (clusters) where intra-cluster similarity is maximized (predominantly positive) and inter-cluster similarity is minimized (predominantly negative). This problem has numerous real-world applications (Tang et al., 2016), particularly in social networks, where vertices represent individuals and edges capture friendly or antagonistic relationships (e.g., shared or opposing political views). Detecting conflicting groups in such networks is crucial for analyzing polarization (Adamic and Glance, 2005; Yardi and Boyd, 2010; Xiao et al., 2020), echo chambers (Garrett, 2009; Flaxman et al., 2016), and the spread of misinformation (Shu et al., 2017; Cooke, 2018; Yang et al., 2019).

In the SNP problem, the k groups must form a partition of the vertices, meaning every vertex must be included. Spectral methods based on the signed Laplacian have been widely used to tackle this problem (Kunegis et al., 2010; Chiang et al., 2012; Mercado et al., 2019; Cucuringu et al., 2019). Alternatively, formulating SNP explicitly as an optimization problem leads to the well-studied *correlation clustering* (CC) problem (Bansal et al., 2004), which is known to be APX-hard. Consequently, numerous approximation algorithms have been developed (Bansal et al., 2004; Charikar et al., 2005; Demaine et al., 2006; Ailon et al., 2008), with local search methods standing out for their strong performance in both clustering quality and computational efficiency (Thiel et al., 2019; Chehreghani, 2023; Aronsson and Chehreghani, 2024a;b).

The problem formulation of PCD is identical to that of SNP, *except that the k clusters are not required to form a partition of the vertices, allowing some vertices to remain unassigned*. The goal is therefore to only find the dense subgraphs of polarized communities. This accounts for cases where certain vertices are neutral w.r.t. the underlying

conflicting group structure. For example, in a social network with a heated political debate, many users may not engage in the dispute, and their interactions might not align with any specific faction. There is a substantial body of work addressing this problem, but most approaches focus on identifying only two communities (Bonchi et al., 2019; Xiao et al., 2020; Ordozgoiti et al., 2020; Fazzone et al., 2022; Niu and Sariyüce, 2023; Gullo et al., 2024). As a result, they do not easily generalize to arbitrary k . To our knowledge, only two works specifically tackle PCD for arbitrary k . (Chu et al., 2016) formulated the task as a constrained quadratic optimization problem and proposes an efficient algorithm that iteratively refines small subgraphs, avoiding the costly computation of the full adjacency matrix. (Tzeng et al., 2020) introduced a spectral method based on maximizing a discrete Rayleigh quotient, which extends the seminal work of (Bonchi et al., 2019) to accommodate arbitrary k . Their method is known to produce highly imbalanced communities in terms of size (Gullo et al., 2024).

The main contributions of this paper are as follows: (i) We propose a novel formulation for the PCD problem that encourages more balanced communities, addressing a key limitation of (Tzeng et al., 2020). (ii) We demonstrate that this formulation is particularly well-suited for optimization via the block-coordinate Frank-Wolfe algorithm (Frank and Wolfe, 1956; Lacoste-Julien et al., 2013). (iii) We establish a simple yet effective equivalent local search method with a provable convergence rate. (iv) We propose techniques that allow the local search method to scale to large networks. (v) Finally, through extensive experiments, we show that our approach consistently outperforms state-of-the-art baselines.

2 Problem Formulation

We start by introducing the relevant notation, followed by an introduction to correlation clustering (CC), which is connected to our problem. Finally, we present the problem of polarized community discovery (PCD).

2.1 Notation

Consider a signed network $G = (V, E)$, where V is the set of objects and E the set of edges. The weight of an edge $(i, j) \in E$ is represented by the element $A_{i,j} \in \{-1, 0, +1\}$ of an adjacency matrix A . The matrix A is symmetric with zeros on the diagonal, which means $A_{i,j} = A_{j,i}$ and $A_{i,i} = 0$. We use $A_{i,\cdot}$ and $A_{\cdot,j}$ to denote row i and column j of A , respectively. While we restrict all similarities to be in $\{-1, 0, +1\}$ (for clarity), all methods presented in the paper extend to arbitrary similarities in \mathbb{R} . We can decompose the adjacency matrix as $A = A^+ - A^-$ where $A^+ = \max(A, 0)$ and $A^- = \max(-A, 0)$. A clustering with k clusters is denoted $S_{[k]} = \{S_1, \dots, S_k\}$, where each $S_m \subseteq V$ is the set of objects assigned to cluster $m \in [k] = \{1, \dots, k\}$. Let $N_{\text{intra}}^+ = \sum_{m \in [k]} \sum_{i,j \in S_m} A_{i,j}^+$ and $N_{\text{intra}}^- = \sum_{m \in [k]} \sum_{i,j \in S_m} A_{i,j}^-$ be the sum of positive and absolute negative intra-cluster similarities, respectively. Furthermore, let $N_{\text{inter}}^+ = \sum_{m \in [k]} \sum_{p \in [k] \setminus \{m\}} \sum_{i \in S_m} \sum_{j \in S_p} A_{i,j}^+$ and $N_{\text{inter}}^- = \sum_{m \in [k]} \sum_{p \in [k] \setminus \{m\}} \sum_{i \in S_m} \sum_{j \in S_p} A_{i,j}^-$ be the sum of positive and absolute negative inter-cluster similarities, respectively.

2.2 Correlation Clustering

We begin by noting that for CC, unlike PCD to be discussed in the next subsection, a clustering $S_{[k]}$ is a partition of V , meaning $V = \bigcup_{m \in [k]} S_m$ and each S_m is disjoint. A notable feature of CC is its ability to automatically determine the number of clusters based on the similarities encoded in A . However, a variant of this problem has also been studied where the number of clusters, k , is specified as an input (Giotis and Guruswami, 2006). Automatic detection of the number of clusters could be a desirable property of a clustering algorithm. However, constraining the number of clusters to k can act as a form of regularization, and has been shown to produce higher-quality clusters in many scenarios (Chehreghani et al., 2012). Given this, the k -CC problem can be defined as shown below.

Problem 1 (k -CC). *Find a clustering $S_{[k]}$ that maximizes*

$$N_{\text{intra}}^+ - N_{\text{intra}}^- + N_{\text{inter}}^- - N_{\text{inter}}^+. \quad (1)$$

In other words, we want to find a clustering that maximizes the sum of intra-cluster similarities and minimizes the sum of inter-cluster similarities. The following proposition presents alternative objectives equivalent to maximizing Eq. 1. While this is known in the CC literature (Chehreghani, 2013), we include a complete summary here to better contextualize our problem.

Proposition 1. *Problem 1 is equivalent to finding a clustering $S_{[k]}$ that maximizes any one of the four objectives below¹.*

$$N_{\text{intra}}^+ + N_{\text{inter}}^- \quad (2)$$

¹By equivalent, we mean they share all local maxima, including the global maximum.

$$-N_{intra}^- - N_{inter}^+ \tag{3}$$

$$N_{intra}^+ - N_{intra}^- \tag{4}$$

$$N_{inter}^- - N_{inter}^+ \tag{5}$$

Furthermore, maximizing any other combination of the four terms is not equivalent to Problem 1.

All proofs can be found in Appendix A. CC is typically formulated as either maximizing agreements (Eq. 2) or minimizing disagreements (Eq. 3) (Bonchi et al., 2014). It can also be framed in terms of maximizing intra-cluster similarities, referred to as *max correlation* (Eq. 4), or minimizing inter-cluster similarities (Eq. 5). Finally, we can combine all these notions into one single objective (i.e., Eq. 1). CC is an NP-hard problem, leading to the development of numerous approximation algorithms. Existing approximation algorithms maximize one of the five expressions above, leading to differences in clustering performance, computational complexity and theoretical performance guarantees.

2.3 Polarized Community Discovery

The problem of PCD is similar to CC in that the goal is to identify k clusters S_1, \dots, S_k , where the similarity within each cluster is large (and positive) and the similarity between different clusters is small (and negative). However, unlike CC, we also allow objects to remain neutral, introducing an additional *neutral* set S_0 . This means an object can either be assigned to one of the non-neutral clusters S_1, \dots, S_k or designated as neutral by assigning it to S_0 . Assigning an object to S_0 effectively excludes it from influencing the objective function. Specifically, assigning an object $i \in V$ to S_0 is equivalent to setting both row $A_{i,:}$ and column $A_{:,i}$ of the matrix A to zero. Consequently, a clustering $S_{[k]}$ is no longer a partition of V and we have $S_0 = V \setminus \bigcup_{m \in [k]} S_m$ (although all clusters are still disjoint). In our view, the goal of PCD is to extract k non-neutral clusters that are (i) large, (ii) balanced, and (iii) dense. Dense clusters imply that each object should strongly align with its assigned cluster—being highly similar to most objects within its cluster and markedly dissimilar to those in other clusters. Objects lacking a clear association, such as those similar to objects in multiple clusters or those that are inherently neutral (e.g., low-degree objects), should be labeled as neutral by assigning them to S_0 . We notice that a natural trade-off exists between the size of the non-neutral clusters and their density, as very small clusters can achieve high density trivially.

We begin this section by explaining why Eq. 1, which incorporates all relevant terms, must be considered when neutral objects are allowed. Much prior work on PCD also optimize all terms, but often without providing a detailed justification for this choice. The next proposition provides such an intuition.

Proposition 2. *A clustering $S_{[k]}$ with neutral objects $S_0 = V \setminus \bigcup_{m \in [k]} S_m$ that maximizes one of the objectives in Eqs. 1-5 is not guaranteed to maximize any of the other objectives².*

From Proposition 2, we conclude that each term in Eq. 1 provides unique information when neutral objects are allowed, unlike the standard CC problem, where the different objectives are equivalent, as outlined by Proposition 1. This makes Eq. 1 the most reasonable objective for optimization in this context, as it effectively balances all contributing terms. Moreover, since each term captures unique aspects of the PCD problem, it may be beneficial to *weight them differently* to achieve an optimal trade-off. Furthermore, (Bonchi et al., 2019) showed that for $k = 2$, an optimal solution to Eq. 1 consists of no neutral objects, i.e., $S_0 = \emptyset$. While we cannot directly extend this conclusion to $k > 2$ (see proof of Proposition 2), it is evident that even for $k > 2$, an object may be assigned to a non-neutral cluster as long as it marginally improves the objective in Eq. 1, even if it does not maintain the density of the graph induced by non-neutral clusters $S_{[k]}$. In other words, low-degree objects that should ideally remain neutral may be included in non-neutral clusters.

Based on the above discussion, we conclude that (i) it may be beneficial to weight the terms in Eq. 1 differently and (ii) we must encourage the presence of neutral objects by penalizing large/sparse non-neutral clusters. In prior work, these concerns are typically addressed by weighting inter-cluster terms with a parameter $\alpha \in \mathbb{R}$ and normalizing Eq. 1 by the number of non-neutral objects, i.e.,

$$\frac{(N_{intra}^+ - N_{intra}^-) + \alpha(N_{inter}^- - N_{inter}^+)}{\sum_{m \in [k]} |S_m|} \tag{6}$$

If $\alpha = 1/(k - 1)$, Eq. 6 is commonly referred to as *polarity* in prior work and is a well-established objective for PCD (Bonchi et al., 2019; Tzeng et al., 2020). However, as highlighted in (Gullo et al., 2024), maximizing polarity often results in highly imbalanced clustering solutions. In particular, clustering solutions with the same polarity can differ significantly in terms of cluster balance. A concrete example illustrating this issue is provided in Appendix C.

²Unless $k = 2$, in which case Eq. 2 and Eq. 1 are equivalent as established in (Bonchi et al., 2019).

Algorithm 1 Block-coordinate Frank-Wolfe Optimization

- 1: Initialize $\mathbf{x}_{[n]}^{(0)} \in \mathcal{D}^{(1)} \times \mathcal{D}^{(2)} \times \dots \times \mathcal{D}^{(n)}$.
 - 2: **for** $t := 0, \dots, T$ **do**
 - 3: Select a random block $i \in [n]$
 - 4: $\mathbf{x}_i^* := \arg \max_{\mathbf{x}_i \in \mathcal{D}^{(i)}} \mathbf{x}_i \cdot \nabla_i f(\mathbf{x}_{[n]}^{(t)})$
 - 5: Let $\gamma := \frac{2n}{t+2n}$ or optimize γ by line-search
 - 6: $\mathbf{x}_i^{(t+1)} := (1 - \gamma)\mathbf{x}_i^{(t)} + \gamma\mathbf{x}_i^*$
 - 7: **end for**
-

In this paper, we propose an alternative objective that, instead of normalizing by the number of non-neutral objects, incorporates a regularization term by subtracting the sum of squared sizes of the non-neutral clusters³:

$$(N_{\text{intra}}^+ - N_{\text{intra}}^-) + \alpha(N_{\text{inter}}^- - N_{\text{inter}}^+) - \beta \sum_{m \in [k]} |S_m|^2. \tag{7}$$

The third term in Eq. 7 has been previously applied to the minimum cut objective for unsigned networks (Chehreghani, 2023) where in practice, however, they use a different penalty: they shift the pairwise similarities so that the sum of the rows and columns of the similarity matrix becomes zero. In our context (i.e., for the PCD problem), this objective achieves two goals simultaneously: it penalizes the formation of (i) large/sparse and (ii) imbalanced non-neutral clusters. The second property is easy to see, as for a clustering with k clusters and n objects, the term $\sum_{m \in [k]} |S_m|^2$ is minimized when each cluster is assigned $\frac{n}{k}$ objects (i.e., the clusters are perfectly balanced). The parameter $\beta \in \mathbb{R}$ allows us to easily trade-off the size of non-neutral clusters and their density, which is a desirable property in this context as discussed in the beginning of this section. As we will demonstrate in the subsequent sections, maximizing our objective with varying values of β allows us to generate a range of clustering solutions with different cluster sizes and corresponding densities. This enables the selection of a solution that offers the most desirable trade-off, and is absent in the existing methods that are based on Eq. 6. Finally, we introduce regularization as an additive term rather than a normalization for three key reasons: (i) It allows for a flexible trade-off between cluster size and density. (ii) It enables the development of efficient optimization procedures with strong convergence guarantees. (iii) As we will demonstrate, it results in superior performance in practice. We are now ready to formally state our problem.

Problem 2 (k -PCD). Find a clustering $S_{[k]}$ with neutral objects $S_0 = V \setminus \bigcup_{m \in [k]} S_m$ that maximizes Eq. 7.

We start by highlighting the computational complexity of the problem with the following theorem.

Theorem 1. Problem 2 (i.e., k -PCD) is NP-hard.

Theorem 1 underscores the necessity of approximate methods to solve Problem 2.

3 Algorithms

In this section, we demonstrate how our problem can be solved using Frank-Wolfe (FW) optimization (Frank and Wolfe, 1956). Specifically, we consider a variant called block-coordinate FW, which we begin by describing in the next subsection. After this, we establish its equivalence to a straightforward and provably efficient local search procedure. Next, we analyze the convergence rate of this approach. Following that, we propose practical enhancements to improve scalability, enabling the method to handle large problems. Finally, we provide a detailed analysis of the impact of α and β .

3.1 Block-Coordinate Frank-Wolfe Optimization

The Frank-Wolfe (FW) algorithm is one of the earliest methods for nonlinear constrained optimization (Frank and Wolfe, 1956). In recent years, it has regained popularity, particularly in machine learning, due to its scalability (Jaggi, 2013). In this paper, we use a variant of this method called block-coordinate FW (Lacoste-Julien et al., 2013). This method yields a significantly faster optimization procedure while enjoying similar theoretical guarantees. Block-coordinate FW is applied to problems where the feasible domain can be split into blocks $\mathcal{D} = \mathcal{D}^{(1)} \times \dots \times \mathcal{D}^{(n)} \subseteq \mathbb{R}^d$, where each $\mathcal{D}^{(i)} \subseteq \mathbb{R}^{d_i}$ is convex and compact and we have $d = \sum_{i=1}^n d_i$. Let $\mathbf{x}_{[n]}$ denote the concatenation of the variables

³For simplicity, we follow prior work by only weighting the inter-cluster terms.

Algorithm 2 Local Search for PCD

- 1: Randomly assign each object $i \in [n]$ to one of the clusters in $S_{[k]}$, or make it neutral by adding it to S_0
 - 2: **while** not converged **do**
 - 3: Select object $i \in [n]$ uniformly at random
 - 4: Assign object i to a cluster (or make it neutral) which maximally increases our objective in Eq. 7.
 - 5: **end while**
-

$\mathbf{x}_i \in \mathcal{D}^{(i)}$ from all blocks $i \in [n]$. The optimization problem is then

$$\max_{\mathbf{x}_{[n]} \in \mathcal{D}^{(1)} \times \dots \times \mathcal{D}^{(n)}} f(\mathbf{x}_{[n]}), \quad (8)$$

where f is a differentiable function with an L -Lipschitz continuous gradient. This approach is particularly effective when optimizing f w.r.t. the variables in a single block (while keeping other blocks fixed) is simple and efficient. This turns out to be the case for our problem, as will be discussed in the remainder of this section. The method is outlined in Alg. 1, where $\nabla_i f(\mathbf{x}_{[n]})$ represents the gradient of $f(\mathbf{x}_{[n]})$ with respect to block \mathbf{x}_i . When the problem involves only a single block ($n = 1$), Alg. 1 reduces to the standard FW algorithm. We now show how our problem can be turned into an instance of Eq. 8. In the following proposition, we show an alternative way of writing our objective in Eq. 7.

Proposition 3. *Our objective in Eq. 7 can be written as*

$$\sum_{m \in [k]} \sum_{i, j \in S_m} (A_{i,j} - \beta) - \alpha \sum_{m \in [k]} \sum_{p \in [k] \setminus \{m\}} \sum_{\substack{i \in S_m \\ j \in S_p}} A_{i,j}. \quad (9)$$

We observe that the regularization term in Eq. 7 is equivalent to shifting the intra-cluster similarities by $-\beta$. This reformulation proves highly useful for the remainder of this section. We now describe how our problem is well-suited for block-coordinate FW. In our context, each object $i \in [n]$ defines a block. We represent the cluster membership of object i using $\mathbf{x}_i \in \{e_0, \dots, e_k\}$, where e_m (for $m \in \{0, \dots, k\}$) are the standard basis vectors. Each \mathbf{x}_i is a vector of dimension $k + 1$, with index zero indicating membership in the neutral set S_0 . Specifically, if $x_{i0} = 1$, object i is assigned to S_0 . Using this notation, we can now define our objective as follows.

$$f(\mathbf{x}_{[n]}) = \sum_{(i,j) \in E} \sum_{m \in [k]} x_{im} x_{jm} (A_{i,j} - \beta) - \alpha \sum_{(i,j) \in E} \sum_{m \in [k]} \sum_{p \in [k] \setminus \{m\}} x_{im} x_{jp} A_{i,j}. \quad (10)$$

Note that we do not include any terms involving x_{i0} , thereby excluding contributions from neutral objects, as intended. The objective in Eq. 10 remains discrete and is therefore unsuitable for FW optimization. To address this, we relax the problem to make it continuous by allowing soft cluster memberships. Specifically, each $\mathbf{x}_i \in \Delta^{k+1}$, where $\Delta^{k+1} = \{\mathbf{x} \in \mathbb{R}^{k+1} \mid x_m \geq 0, \sum_{m=0}^k x_m = 1\}$ represents the simplex of dimension k . With this relaxation, we can now reformulate the optimization problem as follows.

$$\max_{\mathbf{x}_i \in \Delta^{k+1}, \forall i \in [n]} f(\mathbf{x}_{[n]}) \quad (11)$$

Equation 11 is a specific instance of the block-coordinate FW formulation described in Eq. 8 (where f is non-concave). Consequently, we can apply Alg. 1 to solve this problem.

3.2 Equivalence to a Local Search Approach

We now show that optimizing Eq. 11 using Alg. 1 is equivalent to the local search procedure in Alg. 2. Let matrix $G \in \mathbb{R}^{n \times (k+1)}$, where element $G_{i,m} \triangleq [\nabla_i f(\mathbf{x}_{[n]}^{(t)})]_m$ is the gradient of $f(\mathbf{x}_{[n]})$ w.r.t. variable m of block i evaluated at $\mathbf{x}_{[n]}^{(t)}$ (solution at step t of Alg. 1). Given this, we present the following theorem.

Theorem 2. *If $\mathbf{x}_{[n]}^{(0)}$ in Alg 1 is discrete, the following holds. (a) For our problem (Eq. 11), the solution \mathbf{x}_i^* (line 4 of Alg. 1) is the basis vector e_p , where $p = \arg \max_{m \in \{0, \dots, k\}} G_{i,m}$ and the optimal value of the step size on line 6 is $\gamma = 1$. (b) Our objective function in Eq. 10 satisfies $(\mathbf{x}_i^* - \mathbf{x}_i^{(t)}) \cdot G_{i,:} = f(\mathbf{x}_{[n]}^*) - f(\mathbf{x}_{[n]}^{(t)})$, where $\mathbf{x}_{[n]}^*$ is $\mathbf{x}_{[n]}^{(t)}$ with block i modified to \mathbf{x}_i^* .*

From part (a) of Theorem 2, the current solution, $\mathbf{x}_{[n]}^{(t)}$, remains discrete (i.e., hard cluster assignments) at every step of Alg. 1 for all $i \in [n]$. Moreover, each step of Alg. 1 consists of placing object i in the cluster $m \in \{0, \dots, k\}$ with maximal gradient $G_{i,m}$. By part (b) of Theorem 2, this is equivalent to placing object i in the cluster that maximally improves our objective in Eq. 7. Based on this, we conclude the following corollary.

Corollary 1. *From Theorem 2, if $\mathbf{x}_{[n]}^{(0)}$ is discrete, solving the optimization problem in Eq. 11 using Alg. 1 is equivalent to executing the local search procedure described in Alg. 2.*

Given this, we now present results for the convergence rate of Alg. 2.

3.3 Convergence Analysis

Following the prior work on the analysis of general FW algorithms (Jaggi, 2013; Lacoste-Julien et al., 2013), we begin by providing the following definitions.

Definition 1 (FW duality gap). The FW duality gap is defined as (Jaggi, 2013)

$$g(\mathbf{x}_{[n]}) = \max_{\mathbf{s}_{[n]} \in \mathcal{D}} (\mathbf{s}_{[n]} - \mathbf{x}_{[n]}) \cdot \nabla f(\mathbf{x}_{[n]}), \quad (12)$$

which is zero if and only if $\mathbf{x}_{[n]}$ is a stationary point. Furthermore, let $\tilde{g}_t = \min_{0 \leq l \leq t-1} g(\mathbf{x}_{[n]}^{(l)})$ be the smallest duality gap observed in Alg. 1 up until step t .

Definition 2 (Convergence rate). We say the convergence rate of Alg. 1 is at least $O(1/r_t)$ if $\mathbb{E}[\tilde{g}_t] \leq O(1/r_t)$, where r_t is some expression involving only t and the expectation is w.r.t. the random selection of blocks on line 3. If $n = 1$ the bound is deterministic.

The FW algorithm has been shown to converge to a stationary point of f under various settings, with well-established convergence rates. We summarize a few known results below. The standard FW algorithm ($n = 1$) achieves a deterministic convergence rate of $O(1/t)$ for concave f (Frank and Wolfe, 1956) and $O(1/\sqrt{t})$ for non-concave f (Lacoste-Julien, 2016; Reddi et al., 2016). For the block variant, (Lacoste-Julien et al., 2013) prove a convergence rate of $O(1/t)$ for concave f in expectation. For non-concave f , (Thiel et al., 2019) prove a convergence rate of $O(1/t)$ in expectation, under the assumption that $f(\mathbf{x}_{[n]})$ is multilinear in each block \mathbf{x}_i including correlation clustering. We here extend the analysis of (Thiel et al., 2019) to Problem 2 (k -PCD) using Alg. 2, described in Theorem 3. Note that their analysis cannot be applied directly to our objective function in Eq. 10 as this objective does not satisfy the multilinearity property.

Theorem 3. *The convergence rate of Alg. 2 is at least $nh_0/t = O(1/t)$, where $h_0 = \sum_{(i,j) \in E} |A_{i,j}|$.*

The $O(1/t)$ convergence rate presented in Theorem 3 should be compared with the deterministic convergence rate of $O(1/\sqrt{t})$ for general non-concave functions f under the standard FW method ($n = 1$) (Lacoste-Julien, 2016; Reddi et al., 2016).

3.4 Improving the Computational Complexity

In the previous section, we demonstrated that Alg. 2 is guaranteed to converge at the linear rate $O(1/t)$, making it highly efficient. In this section, we propose an alternative version of Alg. 2, designed to enhance the efficiency of each step t while maintaining full equivalence in functionality. This ensures that the convergence analysis from the previous section still remains valid. Firstly, a naive implementation of Alg. 2 has a complexity of $O(Tk^2n^2)$, as each iteration requires $O(k^2n^2)$ to compute the full objective in Eq. 9 for every candidate cluster in order to determine the best cluster for the current object i . Since the number of iterations T until convergence is typically larger than n , this approach can become computationally expensive.

Part (b) of Theorem 2 offers an alternative: *instead of evaluating the full objective, we can compute the gradient $G_{i,:}$, which involves only terms related to object i .* Let $M_{i,m} \triangleq 2 \sum_{j \in S_m} A_{i,j}$, $\eta_i \triangleq \sum_{m \in [k]} M_{i,m}$ and $\beta_{im} = 2\beta|S_m| - 2\beta\mathbf{1}_{[i \in S_m]}$. Given this, we present the following theorem.

Theorem 4. *Let $S_{[k]}$ be the current clustering of our local search procedure, with neutral objects $S_0 = V \setminus \bigcup_{m \in [k]} S_m$. The gradient can then be expressed as follows.*

$$G_{i,m} = -\beta + (1 + \alpha)M_{i,m} - \beta_{im} - \alpha\eta_i \quad (13)$$

for all $m \in [k]$ and $G_{i,0} = 0$.

A naive calculation of the full gradient $G_{i,:}$ for block i is $O(k^2n)$. However, the particular form of the gradient presented in Eq. 13 makes it $O(kn)$. See the proof of Theorem 4 for further insight on this. From Theorem 2, the gradient $G_{i,m}$ represents the impact on the full objective in Eq. 9 if object i is placed in cluster m . Thus, because $G_{i,0} = 0$, we observe that an object i is made neutral if its contribution to all non-neutral clusters is currently negative. Moreover,

Algorithm 3 Local Search for PCD (efficient)

- 1: Randomly assign each object $i \in [n]$ to one of the clusters in $S_{[k]}$, or make it neutral by adding it to S_0
 - 2: Initialize X based on initial clustering $S_{[k]}$
 - 3: $M := 2AX$
 - 4: **while** not converged **do**
 - 5: Select object $i \in [n]$ uniformly at random
 - 6: $\hat{p} :=$ current cluster of i
 - 7: $\eta_i := \sum_p M_{i,p}$
 - 8: $G_{i,p} := -\beta + (1 + \alpha)M_{i,p} - 2\beta|S_p| + 2\beta\mathbf{1}_{[i \in S_p]} - \alpha\eta_i, \forall p \in [k]$
 - 9: $G_{i,0} := 0$
 - 10: $p^* := \arg \max_{p \in \{0, \dots, k\}} G_{i,p}$
 - 11: If $p^* = \hat{p}$, then skip to next iteration
 - 12: Assign object i to cluster S_{p^*}
 - 13: **if** $\hat{p} \in [k]$ (current cluster non-neutral) **then**
 - 14: $M_{:, \hat{p}} := M_{:, \hat{p}} - 2A_{:, i}$
 - 15: **end if**
 - 16: **if** $p^* \neq 0$ (new cluster not neutral) **then**
 - 17: $M_{:, p^*} := M_{:, p^*} + 2A_{:, i}$
 - 18: **end if**
 - 19: **end while**
-

the total complexity is now reduced to $O(Tkn)$, which is a significant improvement over the naive approach with complexity of $O(Tk^2n^2)$.

We present a third approach, outlined in Alg. 3, where we define a matrix $X \in \{0, 1\}^{n \times k}$, with $X_{i,m} = 1$ if object i belongs to cluster $m \in [k]$, and zero otherwise. Neutral objects $i \in S_0$ have rows $X_{i,:}$ of zeros. The procedure precomputes the matrix $M = 2AX$, where $M_{i,m}$ is the total similarity of object i to cluster m . Precomputing M takes $O(kn^2)$, but allows gradient computation in $O(k)$ (line 8). We then have to update $M_{i,m}$ accordingly (lines 15 and 18), which is $O(n)$, reducing the per-iteration complexity to $O(n + k)$. Thus, the total complexity is $O(kn^2 + T(n + k))$, which improves on the $O(Tnk)$ approach because, (i) computing M involves a sparse matrix product, which is highly efficient in practice, and (ii) since $T > n$, reducing per-iteration cost leads to significant practical gains.

3.5 Impact of α and β

We now analyze the impact of α and β in Eq. 7. We begin by stating the following proposition.

Proposition 4. (a) *There exists a $\xi_1 < 0$ such that for any $\beta \leq \xi_1$, there is a clustering solution maximizing Eq. 7 where all the objects are assigned to a single non-neutral cluster. (b) Conversely, there exists a $\xi_2 > 0$ such that for any $\beta \geq \xi_2$, there is a clustering solution maximizing Eq. 7 where all the objects are neutral.*

From Proposition 4, we understand the extreme cases of β : (a) a small negative β results in a maximally imbalanced non-neutral clustering (i.e., all objects in one non-neutral cluster), while (b) a large positive β makes all objects neutral. For intermediate $\beta \in [\xi_1, \xi_2]$, we analyze the gradient in Eq. 13. Increasing β strictly reduces the contribution of object i to each cluster $m \in [k]$, but since the term $-2\beta|S_m|$ scales with cluster size, larger clusters become less favorable, promoting balance. If β is large enough, it forces $G_{i,m} < 0$ for all $m \in [k]$, making neutrality optimal for object i . Note that this is more likely for low-degree objects, implying that high-degree objects (with clear cluster assignment) are more likely to remain non-neutral, resulting in dense non-neutral clusters. Consequently, increasing β leads to smaller (i.e., more neutral objects) and denser non-neutral clusters, while maintaining balanced, as desired.

The parameter α has been studied in prior work (Chu et al., 2016; Tzeng et al., 2020). From Eq. 7, α balances maximizing intra-similarities and minimizing inter-similarities, which translates to a trade-off between cohesion within clusters and separation between them. A heuristic choice of $\alpha = 1/(k - 1)$ was proposed in (Tzeng et al., 2020), based on the observation that the number of intra-similarities scale linearly with k , while the number of inter-similarities grow quadratically. This choice prevents inter-similarities from dominating the objective. Finally, the term $-\alpha\eta_i$ indicates that α influences whether object i becomes neutral, underscoring the need to account for inter-similarities in the objective (as suggested in Section 2.3).

Table 1: Results for different methods and real-world datasets w.r.t. *balance-aware polarity*. $|E|$ is number of non-zero edges. Dashes indicate the method exceeded memory capacity. LSPCD (ours) yields the best results in most of the cases.

		W8	BTC	WIKIV	REF	SD	WIKIC	EP	WIKIP
	$ V $	790	5.9K	7.1K	10.9K	82.1K	116.7K	131.6K	138.6K
	$ E $	116K	214.5K	1M	251.4K	500.5K	2M	711.2K	715.9K
$k = 4$	LSPCD (OURS)	6.9	3.6	5.9	3.9	6.7	26.3	14.9	5.4
	SCG-MA	5.8	0.3	0.8	0.3	1.9	0.7	0.1	0.7
	SCG-MO	4.9	0.3	0.4	0.4	0.2	6.6	0.1	0.0
	SCG-B	0.3	0.1	0.2	0.1	0.5	18.5	0.2	0.1
	SCG-R	1.3	0.9	0.9	0.6	2.4	2.0	0.3	1.0
	KOCG-TOP-1	5.8	4.2	1.2	2.6	0.9	0.4	4.0	0.9
	KOCG-TOP- r	5.4	2.7	2.6	1.6	1.0	2.8	5.9	1.2
	BNC- $(k + 1)$	-0.1	-0.8	-0.4	-1.0	—	—	—	—
	BNC- k	0.5	0.0	0.0	0.0	—	—	—	—
	SPONGE- $(k + 1)$	22.9	0.0	0.4	0.3	—	—	—	—
	SPONGE- k	18.6	0.0	0.0	0.0	—	—	—	—
$k = 6$	LSPCD (OURS)	4.4	2.2	3.6	2.2	3.8	16.4	6.8	3.5
	SCG-MA	3.1	0.1	0.2	0.1	0.0	0.6	0.4	0.0
	SCG-MO	3.6	0.1	0.2	0.1	0.1	4.2	0.1	0.0
	SCG-B	0.3	0.2	0.2	0.1	0.2	1.8	0.2	0.1
	SCG-R	0.3	0.3	0.4	0.2	0.4	2.3	0.1	0.0
	KOCG-TOP-1	6.1	1.7	2.5	3.3	1.7	0.4	2.7	3.7
	KOCG-TOP- r	5.0	1.2	1.8	2.5	1.3	1.1	2.8	0.7
	BNC- $(k + 1)$	-0.1	-0.1	-0.8	-0.4	—	—	—	—
	BNC- k	0.5	0.0	0.0	0.0	—	—	—	—
	SPONGE- $(k + 1)$	17.7	0.0	0.4	0.6	—	—	—	—
	SPONGE- k	16.0	0.0	0.0	0.0	—	—	—	—

4 Experiments

In this section, we describe our experimental studies, where extensive additional results are presented in Appendix B. We use eight publically available datasets, which are commonly used in previous work for PCD. In Appendix B.1, we provide details about each dataset. We compare our efficient local search method for PCD, called LSPCD, against a number of baselines introduced below.

Baselines. (i) SCG (Tzeng et al., 2020) is a spectral method that identifies k non-neutral clusters by maximizing polarity (Eq. 6) with $\alpha = 1/(k - 1)$. It solves a continuous relaxation and applies one of four rounding techniques, resulting in SCG-MA, SCG-R, SCG-MO, and SCG-B. We refer to (Tzeng et al., 2020) for details. (ii) KOCG (Chu et al., 2016) optimizes a similar objective and formulates it as a constrained quadratic optimization problem (this optimization approach is very different from ours). It outputs a set of local minima. For comparison, we select KOCG-top-1 (the best local minimum) and KOCG-top- r , where r is chosen such that the number of non-neutral objects is closest to SCG-MA, following (Tzeng et al., 2020). (iii) BNC (Chiang et al., 2012) and SPONGE (Cucuringu et al., 2019) are spectral methods designed for SNP that do not explicitly handle neutral objects. As in (Tzeng et al., 2020), we apply two heuristics with these methods: (a) we treat all k clusters as non-neutral, and (b) we run the methods with $k + 1$ clusters and then designate the largest cluster as neutral. These variants are denoted BNC- k / SPONGE- k and BNC- $(k + 1)$ / SPONGE- $(k + 1)$, respectively. We use publicly available implementations of these baselines, with further details, including hyperparameters, provided in Appendix B.2.

Metrics. (i) Following prior work, we use *polarity* to evaluate the quality of different methods (Bonchi et al., 2019; Tzeng et al., 2020), defined as in Eq. 6 with $\alpha = 1/(k - 1)$. We note that SCG (Tzeng et al., 2020) explicitly optimizes for polarity, unlike our approach, which gives it an inherent advantage in polarity-based comparisons. (ii) We introduce *balance-aware polarity* (BA-Polarity), which multiplies polarity by a balance factor $|S_m|/|S_l|$, where $|S_m|$ and $|S_l|$ are the sizes of the smallest and largest non-neutral clusters, respectively. In Appendix B.3, we provide a detailed presentation of the solutions found by each method. This includes the number of non-neutral objects identified, the balance of the non-neutral clusters, the runtime, and more.

Results. Tables 1 and 2 present results for different methods and datasets with $k = 4$ and $k = 6$, evaluating BA-Polarity and polarity, respectively. The spectral clustering methods, BNC and SPONGE, exceeded memory limits on large

Table 2: Results for different methods and real-world datasets w.r.t. *polarity*. LSPCD (ours) yields the best or close to the best results. $|E|$ is number of non-zero edges. Dashes indicate the method exceeded memory capacity. LSPCD (ours) yields the best results in most of the cases.

		W8	BTC	WIKIV	REF	SD	WIKIC	EP	WIKIP
	$ V $	790	5.9K	7.1K	10.9K	82.1K	116.7K	131.6K	138.6K
	$ E $	116K	214.5K	1M	251.4K	500.5K	2M	711.2K	715.9K
$k = 4$	LSPCD (OURS)	218.5	23.3	52.6	139.2	61.1	113.6	111.5	71.6
	SCG-MA	205.1	25.1	52.9	94.5	35.5	104.9	127.4	56.5
	SCG-MO	213.2	25.3	53.1	82.1	38.5	117.9	129.0	39.7
	SCG-B	211.6	12.4	24.8	116.2	48.3	49.8	94.4	45.7
	SCG-R	214.6	8.0	19.5	118.7	10.7	41.1	65.1	33.7
	KOCCG-TOP-1	9.1	8.4	4.5	15.0	2.6	4.5	8.9	3.1
	KOCCG-TOP- r	7.4	5.0	3.3	3.7	3.0	3.8	11.0	4.4
	BNC- $(k + 1)$	-0.2	-9.4	-1.1	-1.0	—	—	—	—
	BNC- k	185.3	5.2	15.8	41.5	—	—	—	—
	SPONGE- $(k + 1)$	53.8	1.1	1.0	1.0	—	—	—	—
	SPONGE- k	71.2	5.1	15.8	41.5	—	—	—	—
$k = 6$	LSPCD (OURS)	217.3	20.0	46.2	137.6	57.1	96.1	103.4	58.7
	SCG-MA	207.3	14.6	45.5	84.9	37.8	102.6	88.8	57.5
	SCG-MO	205.8	15.2	47.0	55.6	34.6	111.6	129.2	41.8
	SCG-B	211.6	9.3	23.3	116.2	47.7	46.1	94.5	46.0
	SCG-R	201.2	6.9	10.4	50.3	7.9	18.3	43.3	3.3
	KOCCG-TOP-1	7.9	4.1	4.5	8.6	3.6	4.9	6.0	10.1
	KOCCG-TOP- r	9.1	3.6	3.1	4.0	3.3	1.5	6.8	3.6
	BNC- $(k + 1)$	-0.2	-4.2	-1.1	-0.8	—	—	—	—
	BNC- k	185.2	5.2	15.8	41.5	—	—	—	—
	SPONGE- $(k + 1)$	47.8	1.3	1.0	1.0	—	—	—	—
	SPONGE- k	57.9	5.1	15.8	41.5	—	—	—	—

datasets (caused by k -means), indicated by dashes. Unlike most prior work, which primarily focuses on $k = 2$, we consider more than two clusters; however, for completeness, results for $k = 2$ are provided in Appendix B.3, where similar trends are observed. We report the mean over five runs with different seeds, with standard deviations included in Appendix B.3. For our method, we select the β value that maximizes *polarity*, testing 10 values per dataset, while we fix $\alpha = 1/(k - 1)$ for all methods unless stated otherwise. Results show that our method is highly competitive—often the best—in polarity across all datasets, despite SCG explicitly optimizing for polarity while our method does not. Moreover, our method consistently outperforms all baselines in BA-Polarity. While SCG remains competitive in polarity, our method surpasses it in BA-Polarity across all datasets. In contrast, KOCCG and SPONGE occasionally achieve higher BA-Polarity but at the cost of extremely low polarity (see Table 2) due to overly balanced clustering solutions (arguably to an excessive degree). This demonstrates that our method finds high-polarity solutions while maintaining balance, effectively addressing SCG’s tendency to produce highly imbalanced clusters. Additionally, our method does not impose strict balance constraints, which is beneficial since real-world clusterings are rarely perfectly balanced. Instead, it identifies high-polarity solutions with reasonable balance, making it more practical for real-world applications (further discussed in Appendix B.3).

Figure 1 shows the effect of varying β . Very small or large β values lead to poorer polarity, as they produce clustering solutions with too many or too few of non-neutral objects, respectively. In contrast, intermediate β values yield competitive polarity while consistently outperforming baselines in BA-Polarity. Further insights on the impact of β and α are provided in Appendix B.3, along with other results.

5 Conclusion

We proposed a novel formulation for the polarized community discovery problem, emphasizing (i) large, (ii) dense, and (iii) balanced clustering solutions. We developed an efficient and effective local search method and established its connection to block-coordinate Frank-Wolfe optimization, proving a linear convergence rate of $O(1/t)$. Our extensive experimental results demonstrate that our method achieves high-polarity clustering solutions while maintaining balance, and outperforms the other methods.

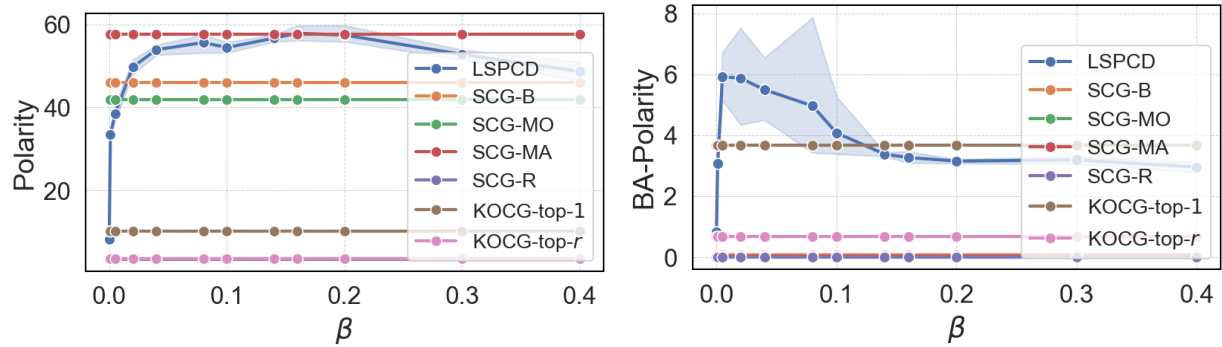


Figure 1: Impact of β on the WikiPol dataset with $k = 6$.

Acknowledgments

This work was partially supported by the Wallenberg AI, Autonomous Systems and Software Program (WASP) funded by the Knut and Alice Wallenberg Foundation.

References

- Frank Harary. On the notion of balance of a signed graph. *Michigan Mathematical Journal*, 2(2):143 – 146, 1953. doi: 10.1307/mmj/1028989917. URL <https://doi.org/10.1307/mmj/1028989917>.
- Jiliang Tang, Yi Chang, Charu C. Aggarwal, and Huan Liu. A survey of signed network mining in social media. *ACM Comput. Surv.*, 49(3):42:1–42:37, 2016. doi: 10.1145/2956185. URL <https://doi.org/10.1145/2956185>.
- Francesco Bonchi, Edoardo Galimberti, Aristides Gionis, Bruno Ordozgoiti, and Giancarlo Ruffo. Discovering polarized communities in signed networks. In Wenwu Zhu, Dacheng Tao, Xueqi Cheng, Peng Cui, Elke A. Rundensteiner, David Carmel, Qi He, and Jeffrey Xu Yu, editors, *Proceedings of the 28th ACM International Conference on Information and Knowledge Management, CIKM 2019, Beijing, China, November 3-7, 2019*, pages 961–970. ACM, 2019. doi: 10.1145/3357384.3357977. URL <https://doi.org/10.1145/3357384.3357977>.
- Ruo-Chun Tzeng, Bruno Ordozgoiti, and Aristides Gionis. Discovering conflicting groups in signed networks. In Hugo Larochelle, Marc’Aurelio Ranzato, Raia Hadsell, Maria-Florina Balcan, and Hsuan-Tien Lin, editors, *Advances in Neural Information Processing Systems 33: Annual Conference on Neural Information Processing Systems 2020, NeurIPS 2020, December 6-12, 2020, virtual*, 2020. URL <https://proceedings.neurips.cc/paper/2020/hash/7cc538b1337957dae283c30ad46def38-Abstract.html>.
- Lada A. Adamic and Natalie Glance. The political blogosphere and the 2004 u.s. election: divided they blog. In *Proceedings of the 3rd International Workshop on Link Discovery, LinkKDD ’05*, page 36–43, New York, NY, USA, 2005. Association for Computing Machinery. ISBN 1595932151. doi: 10.1145/1134271.1134277. URL <https://doi.org/10.1145/1134271.1134277>.
- Sarita Yardi and Danah Boyd. Dynamic debates: An analysis of group polarization over time on twitter. *Bulletin of Science, Technology & Society*, 30(5):316–327, 2010. doi: 10.1177/0270467610380011. URL <https://doi.org/10.1177/0270467610380011>.
- Han Xiao, Bruno Ordozgoiti, and Aristides Gionis. Searching for polarization in signed graphs: a local spectral approach. In Yennun Huang, Irwin King, Tie-Yan Liu, and Maarten van Steen, editors, *WWW ’20: The Web Conference 2020, Taipei, Taiwan, April 20-24, 2020*, pages 362–372. ACM / IW3C2, 2020. doi: 10.1145/3366423.3380121. URL <https://doi.org/10.1145/3366423.3380121>.
- R. Kelly Garrett. Echo chambers online?: Politically motivated selective exposure among internet news users1. *Journal of Computer-Mediated Communication*, 14(2):265–285, 01 2009. ISSN 1083-6101. doi: 10.1111/j.1083-6101.2009.01440.x. URL <https://doi.org/10.1111/j.1083-6101.2009.01440.x>.
- Seth Flaxman, Sharad Goel, and Justin M. Rao. Filter bubbles, echo chambers, and online news consumption. *Public Opinion Quarterly*, 80(S1):298–320, 03 2016. ISSN 0033-362X. doi: 10.1093/poq/nfw006. URL <https://doi.org/10.1093/poq/nfw006>.

- Kai Shu, Amy Sliva, Suhang Wang, Jiliang Tang, and Huan Liu. Fake news detection on social media: A data mining perspective. *SIGKDD Explor.*, 19(1):22–36, 2017. doi: 10.1145/3137597.3137600. URL <https://doi.org/10.1145/3137597.3137600>.
- Nicole A. Cooke. *Fake news and alternative Facts : information literacy in a post-truth era*. ALA Editions special reports. ALA Editions, Chicago, 2018. ISBN 9780838916360.
- Shuo Yang, Kai Shu, Suhang Wang, Renjie Gu, Fan Wu, and Huan Liu. Unsupervised fake news detection on social media: A generative approach. In *The Thirty-Third AAAI Conference on Artificial Intelligence, AAAI 2019, The Thirty-First Innovative Applications of Artificial Intelligence Conference, IAAI 2019, The Ninth AAAI Symposium on Educational Advances in Artificial Intelligence, EAAI 2019, Honolulu, Hawaii, USA, January 27 - February 1, 2019*, pages 5644–5651. AAAI Press, 2019. doi: 10.1609/AAAI.V33i01.33015644. URL <https://doi.org/10.1609/aaai.v33i01.33015644>.
- Jérôme Kunegis, Stephan Schmidt, Andreas Lommatzsch, Jürgen Lerner, Ernesto William De Luca, and Sahin Albayrak. Spectral analysis of signed graphs for clustering, prediction and visualization. In *Proceedings of the SIAM International Conference on Data Mining, SDM 2010, April 29 - May 1, 2010, Columbus, Ohio, USA*, pages 559–570. SIAM, 2010. doi: 10.1137/1.9781611972801.49. URL <https://doi.org/10.1137/1.9781611972801.49>.
- Kai-Yang Chiang, Joyce Jiyoungh Whang, and Inderjit S. Dhillon. Scalable clustering of signed networks using balance normalized cut. In Xue-wen Chen, Guy Lebanon, Haixun Wang, and Mohammed J. Zaki, editors, *21st ACM International Conference on Information and Knowledge Management, CIKM'12, Maui, HI, USA, October 29 - November 02, 2012*, pages 615–624. ACM, 2012. doi: 10.1145/2396761.2396841. URL <https://doi.org/10.1145/2396761.2396841>.
- Pedro Mercado, Francesco Tudisco, and Matthias Hein. Spectral clustering of signed graphs via matrix power means. In Kamalika Chaudhuri and Ruslan Salakhutdinov, editors, *Proceedings of the 36th International Conference on Machine Learning, ICML 2019, 9-15 June 2019, Long Beach, California, USA*, volume 97 of *Proceedings of Machine Learning Research*, pages 4526–4536. PMLR, 2019. URL <http://proceedings.mlr.press/v97/mercado19a.html>.
- Mihai Cucuringu, Peter Davies, Aldo Glielmo, and Hemant Tyagi. SPONGE: A generalized eigenproblem for clustering signed networks. In Kamalika Chaudhuri and Masashi Sugiyama, editors, *The 22nd International Conference on Artificial Intelligence and Statistics, AISTATS 2019, 16-18 April 2019, Naha, Okinawa, Japan*, volume 89 of *Proceedings of Machine Learning Research*, pages 1088–1098. PMLR, 2019. URL <http://proceedings.mlr.press/v89/cucuringu19a.html>.
- Nikhil Bansal, Avrim Blum, and Shuchi Chawla. Correlation clustering. *Mach. Learn.*, 56(1-3):89–113, 2004. doi: 10.1023/B:MACH.0000033116.57574.95. URL <https://doi.org/10.1023/B:MACH.0000033116.57574.95>.
- Moses Charikar, Venkatesan Guruswami, and Anthony Wirth. Clustering with qualitative information. *J. Comput. Syst. Sci.*, 71(3):360–383, 2005. doi: 10.1016/j.jcss.2004.10.012.
- Erik D. Demaine, Dotan Emanuel, Amos Fiat, and Nicole Immorlica. Correlation clustering in general weighted graphs. *Theor. Comput. Sci.*, 361(2-3):172–187, 2006. doi: 10.1016/j.tcs.2006.05.008.
- Nir Ailon, Moses Charikar, and Alantha Newman. Aggregating inconsistent information: Ranking and clustering. *J. ACM*, 55(5):23:1–23:27, 2008. doi: 10.1145/1411509.1411513.
- Erik Thiel, Morteza Haghir Chehreghani, and Devdatt P. Dubhashi. A non-convex optimization approach to correlation clustering. In *The Thirty-Third AAAI Conference on Artificial Intelligence, AAAI 2019, The Thirty-First Innovative Applications of Artificial Intelligence Conference, IAAI 2019, The Ninth AAAI Symposium on Educational Advances in Artificial Intelligence, EAAI 2019, Honolulu, Hawaii, USA, January 27 - February 1, 2019*, pages 5159–5166. AAAI Press, 2019. doi: 10.1609/AAAI.V33i01.33015159. URL <https://doi.org/10.1609/aaai.v33i01.33015159>.
- Morteza Haghir Chehreghani. Shift of pairwise similarities for data clustering. *Mach. Learn.*, 112(6):2025–2051, 2023. doi: 10.1007/S10994-022-06189-6. URL <https://doi.org/10.1007/s10994-022-06189-6>.
- Linus Aronsson and Morteza Haghir Chehreghani. Correlation clustering with active learning of pairwise similarities. *Trans. Mach. Learn. Res.*, 2024, 2024a. URL <https://openreview.net/forum?id=Ryf1TVCjBz>.
- Linus Aronsson and Morteza Haghir Chehreghani. Information-theoretic active correlation clustering, 2024b. URL <https://arxiv.org/abs/2402.03587>.
- Bruno Ordozgoiti, Antonis Matakos, and Aristides Gionis. Finding large balanced subgraphs in signed networks. In Yennun Huang, Irwin King, Tie-Yan Liu, and Maarten van Steen, editors, *WWW '20: The Web Conference 2020, Taipei, Taiwan, April 20-24, 2020*, pages 1378–1388. ACM / IW3C2, 2020. doi: 10.1145/3366423.3380212. URL <https://doi.org/10.1145/3366423.3380212>.

- Adriano Fazzone, Tommaso Lanciano, Riccardo Denni, Charalampos E. Tsourakakis, and Francesco Bonchi. Discovering polarization niches via dense subgraphs with attractors and repulsers. *Proc. VLDB Endow.*, 15(13):3883–3896, 2022. doi: 10.14778/3565838.3565843. URL <https://www.vldb.org/pvldb/vol15/p3883-bonchi.pdf>.
- Jason Niu and Ahmet Erdem Sariyüce. On cohesively polarized communities in signed networks. In Ying Ding, Jie Tang, Juan F. Sequeda, Lora Aroyo, Carlos Castillo, and Geert-Jan Houben, editors, *Companion Proceedings of the ACM Web Conference 2023, WWW 2023, Austin, TX, USA, 30 April 2023 - 4 May 2023*, pages 1339–1347. ACM, 2023. doi: 10.1145/3543873.3587698. URL <https://doi.org/10.1145/3543873.3587698>.
- Francesco Gullo, Domenico Mandaglio, and Andrea Tagarelli. Neural discovery of balance-aware polarized communities. *Mach. Learn.*, 113(9):6611–6644, 2024. doi: 10.1007/S10994-024-06581-4. URL <https://doi.org/10.1007/s10994-024-06581-4>.
- Linyang Chu, Zhefeng Wang, Jian Pei, Jiannan Wang, Zijin Zhao, and Enhong Chen. Finding gangs in war from signed networks. In Balaji Krishnapuram, Mohak Shah, Alexander J. Smola, Charu C. Aggarwal, Dou Shen, and Rajeev Rastogi, editors, *Proceedings of the 22nd ACM SIGKDD International Conference on Knowledge Discovery and Data Mining, San Francisco, CA, USA, August 13-17, 2016*, pages 1505–1514. ACM, 2016. doi: 10.1145/2939672.2939855. URL <https://doi.org/10.1145/2939672.2939855>.
- Marguerite Frank and Philip Wolfe. An algorithm for quadratic programming. *Naval Research Logistics Quarterly*, 3(1-2):95–110, 1956. doi: <https://doi.org/10.1002/nav.3800030109>. URL <https://onlinelibrary.wiley.com/doi/abs/10.1002/nav.3800030109>.
- Simon Lacoste-Julien, Martin Jaggi, Mark Schmidt, and Patrick Pletscher. Block-coordinate frank-wolfe optimization for structural svms. In *Proceedings of the 30th International Conference on Machine Learning, ICML 2013, Atlanta, GA, USA, 16-21 June 2013*, volume 28 of *JMLR Workshop and Conference Proceedings*, pages 53–61. JMLR.org, 2013. URL <http://proceedings.mlr.press/v28/lacoste-julien13.html>.
- Ioannis Giotis and Venkatesan Guruswami. Correlation clustering with a fixed number of clusters. *Theory Comput.*, 2(13):249–266, 2006. doi: 10.4086/TOC.2006.V002A013. URL <https://doi.org/10.4086/toc.2006.v002a013>.
- Morteza Haghir Chehreghani, Alberto Giovanni Busetto, and Joachim M. Buhmann. Information theoretic model validation for spectral clustering. In *Proceedings of the Fifteenth International Conference on Artificial Intelligence and Statistics, AISTATS*, volume 22, pages 495–503, 2012.
- Morteza Haghir Chehreghani. *Information-theoretic validation of clustering algorithms*. PhD thesis, 2013.
- Francesco Bonchi, David García-Soriano, and Edo Liberty. Correlation clustering: from theory to practice. In Sofus A. Macskassy, Claudia Perlich, Jure Leskovec, Wei Wang, and Rayid Ghani, editors, *The 20th ACM SIGKDD International Conference on Knowledge Discovery and Data Mining, KDD '14, New York, NY, USA - August 24 - 27, 2014*, page 1972. ACM, 2014. doi: 10.1145/2623330.2630808. URL <https://doi.org/10.1145/2623330.2630808>.
- Martin Jaggi. Revisiting frank-wolfe: Projection-free sparse convex optimization. In *Proceedings of the 30th International Conference on Machine Learning, ICML 2013, Atlanta, GA, USA, 16-21 June 2013*, volume 28 of *JMLR Workshop and Conference Proceedings*, pages 427–435. JMLR.org, 2013. URL <http://proceedings.mlr.press/v28/jaggi13.html>.
- Simon Lacoste-Julien. Convergence rate of frank-wolfe for non-convex objectives. *CoRR*, abs/1607.00345, 2016. URL <http://arxiv.org/abs/1607.00345>.
- Sashank J. Reddi, Suvrit Sra, Barnabás Póczos, and Alexander J. Smola. Stochastic frank-wolfe methods for nonconvex optimization. In *54th Annual Allerton Conference on Communication, Control, and Computing, Allerton 2016, Monticello, IL, USA, September 27-30, 2016*, pages 1244–1251. IEEE, 2016. doi: 10.1109/ALLERTON.2016.7852377. URL <https://doi.org/10.1109/ALLERTON.2016.7852377>.
- Victor Kristof, Matthias Grossglauser, and Patrick Thiran. War of words: The competitive dynamics of legislative processes. In Yennun Huang, Irwin King, Tie-Yan Liu, and Maarten van Steen, editors, *WWW '20: The Web Conference 2020, Taipei, Taiwan, April 20-24, 2020*, pages 2803–2809. ACM / IW3C2, 2020. doi: 10.1145/3366423.3380041. URL <https://doi.org/10.1145/3366423.3380041>.
- Jure Leskovec and Andrej Krevl. SNAP Datasets: Stanford large network dataset collection. <http://snap.stanford.edu/data>, June 2014.
- Mirko Lai, Viviana Patti, Giancarlo Ruffo, and Paolo Rosso. Stance evolution and twitter interactions in an italian political debate. In Max Silberstein, Faten Atigui, Elena Kornysheva, Elisabeth Métais, and Farid Meziane, editors, *Natural Language Processing and Information Systems - 23rd International Conference on Applications of Natural Language to Information Systems, NLDB 2018, Paris, France, June 13-15, 2018, Proceedings*, volume 10859 of

Lecture Notes in Computer Science, pages 15–27. Springer, 2018. doi: 10.1007/978-3-319-91947-8_2. URL https://doi.org/10.1007/978-3-319-91947-8_2.

Jérôme Kunegis. KONECT: the koblenz network collection. In Leslie Carr, Alberto H. F. Laender, Bernadette Farias Lóscio, Irwin King, Marcus Fontoura, Denny Vrandečić, Lora Aroyo, José Palazzo M. de Oliveira, Fernanda Lima, and Erik Wilde, editors, *22nd International World Wide Web Conference, WWW '13, Rio de Janeiro, Brazil, May 13-17, 2013, Companion Volume*, pages 1343–1350. International World Wide Web Conferences Steering Committee / ACM, 2013. doi: 10.1145/2487788.2488173. URL <https://doi.org/10.1145/2487788.2488173>.

Silviu Maniu, Talel Abdesslem, and Bogdan Cautis. Casting a web of trust over wikipedia: an interaction-based approach. In Sadagopan Srinivasan, Krithi Ramamritham, Arun Kumar, M. P. Ravindra, Elisa Bertino, and Ravi Kumar, editors, *Proceedings of the 20th International Conference on World Wide Web, WWW 2011, Hyderabad, India, March 28 - April 1, 2011 (Companion Volume)*, pages 87–88. ACM, 2011. doi: 10.1145/1963192.1963237. URL <https://doi.org/10.1145/1963192.1963237>.

Ruo-Chun Tzeng. Source code: Discovering conflicting groups in signed networks. <https://github.com/rctzeng/NeurIPS2020-SCG>, 2020.

Lingyang Chu. Source code: Finding gangs in war from signed networks. <https://github.com/lingyangchu/KOCC.SIGKDD2016>, 2016.

Peter Davies and Aldo Glielmo. Signet: A package for clustering of signed networks. <https://github.com/alan-turing-institute/signet>, 2019.

A Proofs

Proposition 1. *Problem 1 is equivalent to finding a clustering $S_{[k]}$ that maximizes any one of the four objectives below⁴.*

$$N_{intra}^+ + N_{inter}^- \quad (2)$$

$$-N_{intra}^- - N_{inter}^+ \quad (3)$$

$$N_{intra}^+ - N_{intra}^- \quad (4)$$

$$N_{inter}^- - N_{inter}^+ \quad (5)$$

Furthermore, maximizing any other combination of the four terms is not equivalent to Problem 1.

Proof. We begin by defining the following quantities, which are constants w.r.t. different clustering solutions for the k -CC problem.

$$c_{sim} \triangleq \sum_{(i,j) \in E} A_{i,j}. \quad (14)$$

$$c_{abs} \triangleq \sum_{(i,j) \in E} |A_{i,j}|. \quad (15)$$

The five objectives can be written as follows.

$$\begin{aligned} f^{full} &\triangleq N_{intra}^+ - N_{intra}^- + N_{inter}^- - N_{inter}^+ = \sum_{m \in [k]} \sum_{i,j \in S_m} A_{i,j} - \sum_{m \in [k]} \sum_{p \in [k] \setminus \{m\}} \sum_{\substack{i \in S_m \\ j \in S_p}} A_{i,j} \\ f^{MaxAgree} &\triangleq N_{intra}^+ + N_{inter}^- \\ &= \sum_{m \in [k]} \sum_{i,j \in S_m} A_{i,j}^+ - \sum_{m \in [k]} \sum_{p \in [k] \setminus \{m\}} \sum_{\substack{i \in S_m \\ j \in S_p}} A_{i,j}^- \\ &= \frac{1}{2} \sum_{m \in [k]} \sum_{i,j \in S_m} (|A_{i,j}| + A_{i,j}) - \frac{1}{2} \sum_{m \in [k]} \sum_{p \in [k] \setminus \{m\}} \sum_{\substack{i \in S_m \\ j \in S_p}} (|A_{i,j}| - A_{i,j}) \\ f^{MinDisagree} &\triangleq N_{intra}^- + N_{inter}^+ \\ &= \sum_{m \in [k]} \sum_{i,j \in S_m} A_{i,j}^- + \sum_{m \in [k]} \sum_{p \in [k] \setminus \{m\}} \sum_{\substack{i \in S_m \\ j \in S_p}} A_{i,j}^+ \\ &= \frac{1}{2} \sum_{m \in [k]} \sum_{i,j \in S_m} (|A_{i,j}| - A_{i,j}) + \frac{1}{2} \sum_{m \in [k]} \sum_{p \in [k] \setminus \{m\}} \sum_{\substack{i \in S_m \\ j \in S_p}} (|A_{i,j}| + A_{i,j}) \\ f^{MaxCorr} &\triangleq N_{intra}^+ - N_{intra}^- = \sum_{m \in [k]} \sum_{i,j \in S_m} A_{i,j} \\ f^{MinCut} &\triangleq -N_{inter}^- + N_{inter}^+ = \sum_{m \in [k]} \sum_{p \in [k] \setminus \{m\}} \sum_{\substack{i \in S_m \\ j \in S_p}} A_{i,j} \end{aligned} \quad (16)$$

Given this, we observe the following connection between the objectives.

⁴By equivalent, we mean they share all local maxima, including the global maximum.

$$\begin{aligned}
 f^{\text{MaxAgree}} &= \frac{1}{2} \sum_{m \in [k]} \sum_{i, j \in S_m} (|A_{i,j}| + A_{i,j}) - \frac{1}{2} \sum_{m \in [k]} \sum_{p \in [k] \setminus \{m\}} \sum_{\substack{i \in S_m \\ j \in S_p}} (|A_{i,j}| - A_{i,j}) \\
 &= \frac{1}{2} f^{\text{full}} + \frac{1}{2} c_{\text{abs}} \\
 &= -f^{\text{MinDisagree}} + c_{\text{abs}} \\
 &= \frac{1}{2} f^{\text{MaxCorr}} - \frac{1}{2} f^{\text{MinCut}} + \frac{1}{2} c_{\text{abs}} \\
 &= f^{\text{MaxCorr}} - \frac{1}{2} c_{\text{sim}} + \frac{1}{2} c_{\text{abs}} \\
 &= -f^{\text{MinCut}} + \frac{1}{2} c_{\text{sim}} + \frac{1}{2} c_{\text{abs}}
 \end{aligned} \tag{17}$$

The above establishes that they are all equal up to constants. We prove the last statement of the proposition by counterexample. We consider the graph $V = \{1, 2, 3\}$ with edge weights $A_{1,2} = +1$, $A_{2,3} = +1$, $A_{1,3} = -1$. The possible clustering solutions (partitions) are:

$$S^{(1)} = \{\{1, 2, 3\}\}, \quad S^{(2)} = \{\{1, 2\}, \{3\}\}, \quad S^{(3)} = \{\{1, 3\}, \{2\}\}, \quad S^{(4)} = \{\{2, 3\}, \{1\}\}, \quad S^{(5)} = \{\{1\}, \{2\}, \{3\}\}.$$

In Table 3, we list all linear combinations of the terms N_{intra}^+ , $-N_{\text{intra}}^-$, N_{inter}^- , $-N_{\text{inter}}^+$ evaluated on each of the five clustering solutions. Expectedly (from the first part of the proposition), the five objectives f^{full} , f^{MaxAgree} , $f^{\text{MinDisagree}}$, f^{MaxCorr} , f^{MinCut} all produce the same ranking of these solutions. In contrast, every other combination of the terms ranks at least one solution differently compared to these five. This proves the last statement of the proposition.

Table 3: All sums of N_{intra}^+ , $-N_{\text{intra}}^-$, N_{inter}^- , $-N_{\text{inter}}^+$ and their values on the five partitions $S^{(m)}$. In parentheses we indicate the known name when the combination corresponds to one of the five standard correlation-clustering objectives (or its negative).

IDX	COMBINATION	$S^{(1)}$	$S^{(2)}$	$S^{(3)}$	$S^{(4)}$	$S^{(5)}$
1	N_{intra}^+	2	1	0	1	0
2	$-N_{\text{intra}}^-$	-1	0	-1	0	0
3	N_{inter}^-	0	1	0	1	1
4	$-N_{\text{inter}}^+$	0	-1	-2	-1	-2
5	$N_{\text{intra}}^+ - N_{\text{intra}}^-$ (f^{MAXCORR})	1	1	-1	1	0
6	$N_{\text{intra}}^+ + N_{\text{inter}}^-$ (f^{MAXAGREE})	2	2	0	2	1
7	$N_{\text{intra}}^+ - N_{\text{inter}}^+$	2	0	-2	0	-2
8	$-N_{\text{intra}}^- + N_{\text{inter}}^-$	-1	1	-1	1	1
9	$-N_{\text{intra}}^- - N_{\text{inter}}^+$ ($-f^{\text{MINDISAGREE}}$)	-1	-1	-3	-1	-2
10	$N_{\text{inter}}^- - N_{\text{inter}}^+$ ($-f^{\text{MINCUT}}$)	0	0	-2	0	-1
11	$N_{\text{intra}}^+ - N_{\text{intra}}^- + N_{\text{inter}}^-$	1	2	-1	2	1
12	$N_{\text{intra}}^+ - N_{\text{intra}}^- - N_{\text{inter}}^+$	1	0	-3	0	-2
13	$N_{\text{intra}}^+ + N_{\text{inter}}^- - N_{\text{inter}}^+$	2	1	-2	1	-1
14	$-N_{\text{intra}}^- + N_{\text{inter}}^- - N_{\text{inter}}^+$	-1	0	-3	0	-1
15	$N_{\text{intra}}^+ - N_{\text{intra}}^- + N_{\text{inter}}^- - N_{\text{inter}}^+$ (f^{FULL})	1	1	-3	1	-1

□

Proposition 2. A clustering $S_{[k]}$ with neutral objects $S_0 = V \setminus \bigcup_{m \in [k]} S_m$ that maximizes one of the objectives in Eqs. 1-5 is not guaranteed to maximize any of the other objectives⁵.

Proof. If an object transitions from neutral to non-neutral, it may introduce agreements (positive intra-cluster or negative inter-cluster similarities) and/or disagreements (negative intra-cluster or positive inter-cluster similarities). An exception

⁵Unless $k = 2$, in which case Eq. 2 and Eq. 1 are equivalent as established in (Bonchi et al., 2019).

is objects with zero degree (zero similarity to all others), which can be assigned as neutral or non-neutral without affecting any of the five objectives. Thus, we only consider non-zero degree objects in the remainder of the proof.

The *max agreement* objective (Eq. 2) considers only agreements. Making an object non-neutral either increases or maintains the objective but never decreases it, ensuring all objects become non-neutral. Conversely, the *min disagreement* objective (Eq. 3) considers only disagreements. Making an object non-neutral either decreases or maintains the objective but never improves it, ensuring all objects remain neutral.

Now, consider a clustering with k non-neutral clusters, where all intra-cluster similarities are $+1$ and all inter-cluster similarities are -1 . If an unassigned object $i \in V$ has similarity $+1$ to all others, the *max correlation* objective (Eq. 4) assigns it to the largest non-neutral cluster, while the *minimum cut* objective (Eq. 5) keeps it neutral. For $k > 2$, the full objective (Eq. 1) places i in the largest non-neutral cluster if its size exceeds the sum of all others; otherwise, it remains neutral. Conversely, if object i has similarity -1 to all others, *max correlation* keeps it neutral, whereas *minimum cut* assigns it to the smallest non-neutral cluster. For $k > 2$, the full objective may assign i as neutral or non-neutral depending on cluster sizes.

Therefore, we conclude that *max agreement* and *min disagreement* differ fundamentally, always assigning all objects as non-neutral or neutral, respectively. Furthermore, from the two counterexamples above, *max correlation*, *minimum cut*, and the full objective are not equivalent and none of them guarantee that all objects are either neutral or non-neutral in all cases (meaning they are all different from *max agreement* and *min disagreement* in general).

For $k = 2$, the full objective always increases (or remains constant) when an object is made non-neutral, aligning it with *max agreement*. To see this, consider a clustering with $k = 2$ non-neutral clusters, and let $M_{i,m} = \sum_{j \in S_m} A_{i,j}$ be the total similarity of object i to cluster m . The impact on the objective when assigning i to m is $M_{i,m} - M_{i,p}$, where p is the other cluster. Since this difference is always positive when i is placed in its most similar cluster, assigning i as non-neutral always improves the objective. Then, since all objects are non-neutral, the problem is equivalent to the k -CC problem where we know *max agreement* and the full objective are equivalent (from Proposition 1). For $k > 2$, this reasoning no longer holds, as contributions from other clusters can outweigh the within-cluster similarity to the most similar cluster (i.e., making the total contribution negative), potentially making neutrality optimal. However, we note that in our final objective (Eq. 7), when α and β are involved, all terms will contribute with unique information even for $k = 2$.

□

Theorem 1. *Problem 2 (i.e., k -PCD) is NP-hard.*

Proof. Fix $\alpha, \beta \in \mathbb{R}$ to any values. Assume that we know which objects in V should be assigned to the neutral set S_0 in the optimal solution to the k -PCD problem. Then, let $V' = V \setminus S_0$ and let E' be the set of edges between objects in V' . Since no object in V' should be neutral, the problem reduces to finding a partition of V' that maximizes Eq. 7. We rewrite our objective in Eq. 7 as

$$\begin{aligned}
 (N_{\text{intra}}^+ - N_{\text{intra}}^-) + \alpha(N_{\text{inter}}^- - N_{\text{inter}}^+) - \beta \sum_{m \in [k]} |S_m|^2 &= \sum_{m \in [k]} \sum_{i,j \in S_m} A_{i,j} - \alpha \sum_{m \in [k]} \sum_{p \in [k] \setminus \{m\}} \sum_{\substack{i \in S_m \\ j \in S_p}} A_{i,j} - \beta \sum_{m \in [k]} |S_m|^2 \\
 &= \sum_{m \in [k]} \sum_{i,j \in S_m} (A_{i,j} - \beta) - \alpha \sum_{m \in [k]} \sum_{p \in [k] \setminus \{m\}} \sum_{\substack{i \in S_m \\ j \in S_p}} A_{i,j}.
 \end{aligned} \tag{18}$$

The second equality follows from Proposition 3. Defining $c_{\text{sim}} \triangleq \sum_{(i,j) \in E'} A_{i,j}$, we obtain:

$$\sum_{m \in [k]} \sum_{p \in [k] \setminus \{m\}} \sum_{\substack{i \in S_m \\ j \in S_p}} A_{i,j} = c_{\text{sim}} - \sum_{m \in [k]} \sum_{i,j \in S_m} A_{i,j}. \tag{19}$$

Substituting this into Eq. 18 and simplifying:

$$\begin{aligned}
 \sum_{m \in [k]} \sum_{i,j \in S_m} (A_{i,j} - \beta) - \alpha \sum_{m \in [k]} \sum_{p \in [k] \setminus \{m\}} \sum_{\substack{i \in S_m \\ j \in S_p}} A_{i,j} &= \sum_{m \in [k]} \sum_{i,j \in S_m} (A_{i,j} - \beta) - \alpha (c_{\text{sim}} - \sum_{m \in [k]} \sum_{i,j \in S_m} A_{i,j}) \\
 &= (1 + \alpha) \sum_{m \in [k]} \sum_{i,j \in S_m} (A_{i,j} - \beta) - \alpha c_{\text{sim}}.
 \end{aligned} \tag{20}$$

Defining $A'_{i,j} = (1 + \alpha)(A_{i,j} - \beta)$, we observe that since c_{sim} is a constant across clustering solutions, the problem reduces to finding a partition of V' that maximizes $\sum_{m \in [k]} \sum_{i,j \in S_m} A'_{i,j}$. This is equivalent to the *max correlation* objective (Eq. 4) applied to the transformed adjacency matrix A' . By Proposition 1, this objective is equivalent to the k -CC problem (Problem 1). Thus, solving the k -PCD problem requires solving the k -CC problem on the instance $G' = (V', E')$, meaning k -PCD is at least as hard as k -CC. Since correlation clustering is NP-hard (Bansal et al., 2004; Giotis and Guruswami, 2006), we conclude that k -PCD is also NP-hard. \square

Proposition 3. *Our objective in Eq. 7 can be written as*

$$\sum_{m \in [k]} \sum_{i,j \in S_m} (A_{i,j} - \beta) - \alpha \sum_{m \in [k]} \sum_{p \in [k] \setminus \{m\}} \sum_{\substack{i \in S_m \\ j \in S_p}} A_{i,j}. \tag{9}$$

Proof. We have

$$\begin{aligned}
 (N_{\text{intra}}^+ - N_{\text{intra}}^-) + \alpha(N_{\text{inter}}^- - N_{\text{inter}}^+) - \beta \sum_{m \in [k]} |S_m|^2 &= \\
 = \sum_{m \in [k]} \sum_{i,j \in S_m} A_{i,j} - \alpha \sum_{m \in [k]} \sum_{p \in [k] \setminus \{m\}} \sum_{\substack{i \in S_m \\ j \in S_p}} A_{i,j} - \beta \sum_{m \in [k]} |S_m|^2 & \\
 = \sum_{m \in [k]} \sum_{i,j \in S_m} A_{i,j} - \alpha \sum_{m \in [k]} \sum_{p \in [k] \setminus \{m\}} \sum_{\substack{i \in S_m \\ j \in S_p}} A_{i,j} - \beta \sum_{m \in [k]} \sum_{i,j \in S_m} 1 & \\
 = \sum_{m \in [k]} \sum_{i,j \in S_m} A_{i,j} - \alpha \sum_{m \in [k]} \sum_{p \in [k] \setminus \{m\}} \sum_{\substack{i \in S_m \\ j \in S_p}} A_{i,j} - \sum_{m \in [k]} \sum_{i,j \in S_m} \beta & \\
 = \sum_{m \in [k]} \sum_{i,j \in S_m} (A_{i,j} - \beta) - \alpha \sum_{m \in [k]} \sum_{p \in [k] \setminus \{m\}} \sum_{\substack{i \in S_m \\ j \in S_p}} A_{i,j}. &
 \end{aligned} \tag{21}$$

The second equality (line 3) holds because the number of pairs of objects inside cluster m is $|S_m|^2$. A similar regularization is established in (Chehreghani, 2023) for the minimum cut objective, where it is shown that optimizing this minimum cut objective regularized with $-\beta \sum_{m \in [k]} |S_m|^2$ is equivalent to optimizing the max correlation objective (Eq. 4) with similarities shifted by β . However, their result specifically considers the full network partitioning of unsigned networks, where the initial pairwise similarities are assumed non-negative. Moreover, they use a different regularization in practice: they shift the pairwise similarities so that the sum of the rows and columns of the similarity matrix becomes zero. \square

Theorem 2. *If $\mathbf{x}_{[n]}^{(0)}$ in Alg 1 is discrete, the following holds. (a) For our problem (Eq. 11), the solution \mathbf{x}_i^* (line 4 of Alg. 1) is the basis vector \mathbf{e}_p , where $p = \arg \max_{m \in \{0, \dots, k\}} G_{i,m}$ and the optimal value of the step size on line 6 is $\gamma = 1$. (b) Our objective function in Eq. 10 satisfies $(\mathbf{x}_i^* - \mathbf{x}_i^{(t)}) \cdot G_{i,:} = f(\mathbf{x}_{[n]}^*) - f(\mathbf{x}_{[n]}^{(t)})$, where $\mathbf{x}_{[n]}^*$ is $\mathbf{x}_{[n]}^{(t)}$ with block i modified to \mathbf{x}_i^* .*

Proof. We begin by writing our objective function $f(\mathbf{x}_{[n]})$ in Eq. 10 as follows.

$$\begin{aligned}
 f(\mathbf{x}_{[n]}) &= \sum_{(i,j) \in E} \sum_{m \in [k]} x_{im} x_{jm} (A_{i,j} - \beta) - \alpha \sum_{(i,j) \in E} \sum_{m \in [k]} \sum_{p \in [k] \setminus \{m\}} x_{im} x_{jp} A_{i,j} \\
 &= - \sum_{i \in [n]} \sum_{m \in [k]} x_{im}^2 \beta + \sum_{\substack{(i,j) \in E \\ i \neq j}} \sum_{m \in [k]} x_{im} x_{jm} (A_{i,j} - \beta) - \alpha \sum_{(i,j) \in E} \sum_{m \in [k]} \sum_{p \in [k] \setminus \{m\}} x_{im} x_{jp} A_{i,j} \\
 &= - \sum_{i \in [n]} \sum_{m \in [k]} x_{im} \beta + \sum_{\substack{(i,j) \in E \\ i \neq j}} \sum_{m \in [k]} x_{im} x_{jm} (A_{i,j} - \beta) - \alpha \sum_{(i,j) \in E} \sum_{m \in [k]} \sum_{p \in [k] \setminus \{m\}} x_{im} x_{jp} A_{i,j}.
 \end{aligned} \tag{22}$$

In the second equality, we separate out the terms for $i = j$ and use that $A_{i,i} = 0$. In the third equality, we consider that $\mathbf{x}_{[n]}$ is a discrete solution. This makes the first term linear instead of being quadratic w.r.t. x_{im} , which is a crucial step in proving the theorem. Let $f(\mathbf{x}_i)$ denote $f(\mathbf{x}_{[n]})$ when treating all blocks other than \mathbf{x}_i as constants. Then,

$$\begin{aligned}
 f(\mathbf{x}_i) &= - \sum_{m \in [k]} x_{im} \beta + 2 \sum_{j \in [n] \setminus \{i\}} \sum_{m \in [k]} x_{im} x_{jm} (A_{i,j} - \beta) - 2\alpha \sum_{j \in [n] \setminus \{i\}} \sum_{m \in [k]} \sum_{p \in [k] \setminus \{m\}} x_{im} x_{jp} A_{i,j} + C \\
 &= \sum_{m \in [k]} x_{im} \left(-\beta + 2 \underbrace{\sum_{j \in [n] \setminus \{i\}} (x_{jm} (A_{i,j} - \beta) - \alpha \sum_{p \in [k] \setminus \{m\}} x_{jp} A_{i,j})}_{c_{im}} \right) + C,
 \end{aligned} \tag{23}$$

where C denotes terms independent of \mathbf{x}_i . Define $\mathbf{c}_i \in \mathbb{R}^{k+1}$ with elements

$$c_{im} \triangleq -\beta + 2 \sum_{j \in [n] \setminus \{i\}} (x_{jm} (A_{i,j} - \beta) - \alpha \sum_{p \in [k] \setminus \{m\}} x_{jp} A_{i,j}), \quad \text{for } m \in [k], \quad c_{i0} \triangleq 0. \tag{24}$$

Then, we obtain

$$f(\mathbf{x}_i) = \sum_{m \in \{0, \dots, k\}} x_{im} c_{im} + C = \mathbf{x}_i^T \mathbf{c}_i + C. \tag{25}$$

Eq. 25 clearly illustrates that the contribution of the neutral component (index zero) of each x_{im} is not included in the total objective (since $c_{i0} = 0$). From Eq. 25, the gradient of $f(\mathbf{x}_{[n]})$ w.r.t. \mathbf{x}_i is

$$\nabla_i f(\mathbf{x}_{[n]}) = \mathbf{c}_i. \tag{26}$$

Let $\mathbf{c}_i^{(t)} = \nabla_i f(\mathbf{x}_{[n]}^{(t)})$ be the gradient of $f(\mathbf{x}_{[n]})$ evaluated at the current solution $\mathbf{x}_{[n]}^{(t)}$ (defined as in Eq. 24). The optimization problem on line 4 of Algorithm 1 is

$$\mathbf{x}_i^* = \arg \max_{\mathbf{x}_i \in \Delta^{k+1}} \mathbf{x}_i^T \mathbf{c}_i^{(t)}. \tag{27}$$

Since Eq. 27 is a linear program over the simplex Δ^{k+1} , the optimal solution is obtained by setting $x_{im}^* = 1$ for $m = \arg \max_{m \in \{0, \dots, k\}} c_{im}^{(t)}$ and $x_{ip}^* = 0$ for all $p \neq m$. This proves the first statement of part (a) of the theorem.

Next, we note that the difference $f(\mathbf{x}_{[n]}^*) - f(\mathbf{x}_{[n]}^{(t)})$ simplifies to $f(\mathbf{x}_i^*) - f(\mathbf{x}_i^{(t)})$ (where $f(\mathbf{x}_i)$ is defined in Eq. 23), since only the terms involving the variables in block i change between $\mathbf{x}_{[n]}^*$ and $\mathbf{x}_{[n]}^{(t)}$. Therefore, we can derive the following.

$$\begin{aligned}
 f(\mathbf{x}_{[n]}^*) - f(\mathbf{x}_{[n]}^{(t)}) &= f(\mathbf{x}_i^*) - f(\mathbf{x}_i^{(t)}) \\
 &= ((\mathbf{x}_i^*)^T \mathbf{c}_i^* + C) - ((\mathbf{x}_i^{(t)})^T \mathbf{c}_i^{(t)} + C) \\
 &= ((\mathbf{x}_i^*)^T \mathbf{c}_i^{(t)} + C) - ((\mathbf{x}_i^{(t)})^T \mathbf{c}_i^{(t)} + C) \\
 &= ((\mathbf{x}_i^*)^T - (\mathbf{x}_i^{(t)})^T) \mathbf{c}_i^{(t)} \\
 &= (\mathbf{x}_i^* - \mathbf{x}_i^{(t)}) \cdot \nabla_i f(\mathbf{x}_{[n]}^{(t)})
 \end{aligned} \tag{28}$$

Here, \mathbf{c}_i^* is defined as in Eq. 24 w.r.t. $\mathbf{x}_{[n]}^*$. Since $\mathbf{x}_{[n]}^*$ and $\mathbf{x}_{[n]}^{(t)}$ differ only in block i , and neither \mathbf{c}_i^* nor $\mathbf{c}_i^{(t)}$ depend on the variables in block i , it follows that $\mathbf{c}_i^* = \mathbf{c}_i^{(t)}$, justifying the third equality. In Eq. 22, we assume that $\mathbf{x}_{[n]}$ is discrete. To ensure this property holds throughout, we require that both $\mathbf{x}_{[n]}^*$ and $\mathbf{x}_{[n]}^{(t)}$ remain discrete for all $t \in \{0, \dots, T\}$.

First, by assumption in the theorem, $\mathbf{x}_{[n]}^{(0)}$ is discrete. From part (a), we know that \mathbf{x}_i^* is discrete, implying $\mathbf{x}_{[n]}^*$ is discrete as long as $\mathbf{x}_{[n]}^{(t)}$ is discrete. Furthermore, from Eq. 28, the optimal solution \mathbf{x}_i^* in line 4 of Algorithm 1 maximally increases the objective, which ensures the optimal step size in line 6 is $\gamma = 1$ (proving the second statement of part (a)). Consequently, $\mathbf{x}_i^{(t+1)}$ remains discrete. By induction, this guarantees that $\mathbf{x}_{[n]}^{(t)}$ is discrete for all t , ensuring Eq. 28 holds for all $t \in \{0, \dots, T\}$. This completes the proof of part (b) of the theorem. \square

Theorem 3. *The convergence rate of Alg. 2 is at least $nh_0/t = O(1/t)$, where $h_0 = \sum_{(i,j) \in E} |A_{i,j}|$.*

Proof. From Definition 1, we have that, in our case, the FW duality gap is defined as

$$g(\mathbf{x}_{[n]}) \triangleq \max_{\mathbf{s}_i \in \Delta^{k+1}, \forall i \in [n]} (\mathbf{s}_{[n]} - \mathbf{x}_{[n]}) \cdot \nabla f(\mathbf{x}_{[n]}). \tag{29}$$

Then, we recall that

$$\tilde{g}_t = \min_{0 \leq l \leq t-1} g(\mathbf{x}_{[n]}^{(l)}) \tag{30}$$

is the smallest duality gap observed in Alg. 1 up until step t . As established by (Lacoste-Julien et al., 2013) for general domains, the FW duality gap can be decomposed as follows.

$$\begin{aligned}
 g(\mathbf{x}_{[n]}) &\triangleq \max_{\mathbf{s}_i \in \Delta^{k+1}, \forall i \in [n]} (\mathbf{s}_{[n]} - \mathbf{x}_{[n]}) \cdot \nabla f(\mathbf{x}_{[n]}) \\
 &= \max_{\mathbf{s}_i \in \Delta^{k+1}, \forall i \in [n]} \sum_{i \in [n]} (\mathbf{s}_i - \mathbf{x}_i) \cdot \nabla_i f(\mathbf{x}_{[n]}) \\
 &= \sum_{i \in [n]} \underbrace{\max_{\mathbf{s}_i \in \Delta^{k+1}} (\mathbf{s}_i - \mathbf{x}_i) \cdot \nabla_i f(\mathbf{x}_{[n]})}_{\triangleq g_i(\mathbf{x}_{[n]})}
 \end{aligned} \tag{31}$$

Let $g_i(\mathbf{x}_{[n]}) \triangleq \max_{\mathbf{s}_i \in \Delta^{k+1}} (\mathbf{s}_i - \mathbf{x}_i) \cdot \nabla_i f(\mathbf{x}_{[n]})$ be the duality gap related to block i . We have that the FW duality gap is the sum of the gaps from each block: $g(\mathbf{x}_{[n]}) = \sum_{i \in [n]} g_i(\mathbf{x}_{[n]})$.

From Definition 2 (convergence rate), in order to prove the stated convergence rate, we need to show that $\mathbb{E}[\tilde{g}_t] \leq nh_0/t$. The structure of our proof is similar to the proof of Theorem 2 in (Thiel et al., 2019). However, here we adapt it to our problem and make the proof more rigorous (including correction of a mistake in the proof by (Thiel et al., 2019)). A key difference is that our objective in Eq. 10 is not multilinear in the blocks i . Then, as shown in Eq. 22 of Theorem 2, the first quadratic term can be transformed into a linear one by assuming a discrete solution (which we showed holds at every step t).

In Alg. 1, a block $i \in [n]$ is chosen uniformly at random (on line 3). Therefore, we have

$$\begin{aligned}
 \mathbb{E}[g_i(\mathbf{x}_{[n]}^{(t)})|\mathbf{x}_{[n]}^{(t)}] &= \sum_{i \in [n]} P(i \text{ is selected})g_i(\mathbf{x}_{[n]}^{(t)}) \\
 &= \sum_{i \in [n]} \frac{1}{n}g_i(\mathbf{x}_{[n]}^{(t)}) \\
 &= \frac{1}{n} \sum_{i \in [n]} \max_{\mathbf{s}_i^{(t)} \in \Delta^{k+1}} (\mathbf{s}_i - \mathbf{x}_i^{(t)}) \cdot \nabla_i f(\mathbf{x}_{[n]}^{(t)}) \\
 &= \frac{1}{n}g(\mathbf{x}_{[n]}^{(t)}).
 \end{aligned} \tag{32}$$

We now take an expectation w.r.t. $\mathbf{x}_{[n]}^{(t)}$ on both sides and obtain

$$\begin{aligned}
 \mathbb{E}[\mathbb{E}[g_i(\mathbf{x}_{[n]}^{(t)})|\mathbf{x}_{[n]}^{(t)}]] &= \frac{1}{n}\mathbb{E}[g(\mathbf{x}_{[n]}^{(t)})] \\
 &= \mathbb{E}[g_i(\mathbf{x}_{[n]}^{(t)})],
 \end{aligned} \tag{33}$$

where the last equality follows from the Law of Total Expectation (i.e., that $\mathbb{E}_Y[\mathbb{E}_X[X|Y]] = \mathbb{E}_X[X]$, where X and Y are random variables). We therefore have that $\frac{1}{n}\mathbb{E}[g(\mathbf{x}_{[n]}^{(t)})] = \mathbb{E}[g_i(\mathbf{x}_{[n]}^{(t)})]$, where the expectation is w.r.t. all randomly chosen blocks i before step t . Now, from Theorem 2 we have that our objective satisfies

$$f(\mathbf{x}_{[n]}^{(t+1)}) - f(\mathbf{x}_{[n]}^{(t)}) = g_i(\mathbf{x}_{[n]}^{(t)}) = \max_{\mathbf{s}_i^{(t)} \in \Delta^{k+1}} (\mathbf{s}_i - \mathbf{x}_i^{(t)}) \cdot \nabla_i f(\mathbf{x}_{[n]}^{(t)}). \tag{34}$$

Then, we have

$$\begin{aligned}
 \frac{1}{n} \sum_{t=0}^{T-1} \mathbb{E}[g(\mathbf{x}^{(t)})] &= \sum_{t=0}^{T-1} \mathbb{E}[g_i(\mathbf{x}_{[n]}^{(t)})] \\
 &= \sum_{t=0}^{T-1} \mathbb{E}[f(\mathbf{x}_{[n]}^{(t+1)}) - f(\mathbf{x}_{[n]}^{(t)})] \\
 &= \mathbb{E}[f(\mathbf{x}_{[n]}^{(T)})] - f(\mathbf{x}_{[n]}^{(0)}) \\
 &\leq OPT - f(\mathbf{x}_{[n]}^{(0)}),
 \end{aligned} \tag{35}$$

where the third equality is due to the *telescoping rule* and OPT is the objective value of the optimal clustering solution to Problem 1 (k -PCD). On the other hand, we have

$$\frac{1}{n} \sum_{t=0}^{T-1} \mathbb{E}[g(\mathbf{x}^{(t)})] \geq \frac{T}{n}\mathbb{E}[\tilde{g}_T], \tag{36}$$

where \tilde{g}_t is defined as in Eq. 30 (the smallest gap observed until step t). Therefore,

$$\begin{aligned}
 \frac{T}{n}\mathbb{E}[\tilde{g}_T] &\leq OPT - f(\mathbf{x}^{(0)}) \\
 \Rightarrow \mathbb{E}[\tilde{g}_T] &\leq \frac{n(OPT - f(\mathbf{x}^{(0)}))}{T}.
 \end{aligned} \tag{37}$$

The value of OPT depends on the particular instance. In order to obtain an instance-independent bound, we use that $OPT - f(\mathbf{x}^{(0)}) \leq \sum_{(i,j) \in E} |A_{i,j}|$ resulting in

$$\mathbb{E}[\tilde{g}_T] \leq \frac{n \sum_{(i,j) \in E} |A_{i,j}|}{T}. \tag{38}$$

which we aimed to show since it holds for any T . \square

Corollary 1. *From Theorem 2, if $\mathbf{x}_{[n]}^{(0)}$ is discrete, solving the optimization problem in Eq. 11 using Alg. 1 is equivalent to executing the local search procedure described in Alg. 2.*

Proof. From part (a) of Theorem 2, the current solution, $\mathbf{x}_{[n]}^{(t)}$, remains discrete (i.e., hard cluster assignments) at every step of Alg. 1 for all $i \in [n]$. Moreover, each step of Alg. 1 consists of placing object i in the cluster $m \in \{0, \dots, k\}$ with maximal gradient $G_{i,m}$. By part (b) of Theorem 2, this is equivalent to placing object i in the cluster that maximally improves our objective in Eq. 7. \square

Theorem 4. *Let $S_{[k]}$ be the current clustering of our local search procedure, with neutral objects $S_0 = V \setminus \bigcup_{m \in [k]} S_m$. The gradient can then be expressed as follows.*

$$G_{i,m} = -\beta + (1 + \alpha)M_{i,m} - \beta_{im} - \alpha\eta_i \quad (13)$$

for all $m \in [k]$ and $G_{i,0} = 0$.

Proof. From Theorem 2, we recall that since the current solution $\mathbf{x}_{[n]}^{(t)}$ always remains discrete, our objective can be written as

$$f(\mathbf{x}_{[n]}^{(t)}) = - \sum_{i \in [n]} \sum_{m \in [k]} x_{im}^{(t)} \beta + \sum_{\substack{(i,j) \in E \\ i \neq j}} \sum_{m \in [k]} x_{im}^{(t)} x_{jm}^{(t)} (A_{i,j} - \beta) - \alpha \sum_{(i,j) \in E} \sum_{m \in [k]} \sum_{p \in [k] \setminus \{m\}} x_{im}^{(t)} x_{jp}^{(t)} A_{i,j}. \quad (39)$$

We let $f(\mathbf{x}_i^{(t)})$ denote $f(\mathbf{x}_{[n]}^{(t)})$ when treating all blocks other than $\mathbf{x}_i^{(t)}$ as constants. Then,

$$f(\mathbf{x}_i^{(t)}) = \sum_{m \in [k]} x_{im}^{(t)} \underbrace{\left(-\beta + 2 \sum_{j \in [n] \setminus \{i\}} x_{jm}^{(t)} (A_{i,j} - \beta) - 2\alpha \sum_{j \in [n] \setminus \{i\}} \sum_{p \in [k] \setminus \{m\}} x_{jp}^{(t)} A_{i,j} \right)}_{c_{im}} + C. \quad (40)$$

Therefore, we have

$$G_{i,m} \triangleq [\nabla_i f(\mathbf{x}_{[n]}^{(t)})]_m = c_{im}, \quad \text{for } m \in [k]. \quad (41)$$

This holds because neither c_{im} nor C depend on $x_{im}^{(t)}$. Furthermore, since x_{i0} does not show up in Eq. 40, everything in Eq. 40 is a constant w.r.t. x_{i0} . We therefore have

$$G_{i,0} \triangleq [\nabla_i f(\mathbf{x}_{[n]}^{(t)})]_0 = 0. \quad (42)$$

By noting that $\mathbf{x}^{(t)}$ is discrete, we can rewrite c_{im} for $m \in [k]$ as follows.

$$\begin{aligned} c_{im} &= -\beta + 2 \sum_{j \in [n] \setminus \{i\}} x_{jm}^{(t)} (A_{i,j} - \beta) - 2\alpha \sum_{j \in [n] \setminus \{i\}} \sum_{p \in [k] \setminus \{m\}} x_{jp}^{(t)} A_{i,j} \\ &= -\beta + 2 \sum_{j \in [n] \setminus \{i\}} x_{jm}^{(t)} A_{i,j} - 2 \sum_{j \in [n] \setminus \{i\}} \beta - 2\alpha \sum_{j \in [n] \setminus \{i\}} \sum_{p \in [k] \setminus \{m\}} x_{jp}^{(t)} A_{i,j} \\ &= -\beta + 2 \sum_{j \in S_m \setminus \{i\}} A_{i,j} - 2 \sum_{j \in S_m \setminus \{i\}} \beta - 2\alpha \sum_{p \in [k] \setminus \{m\}} \sum_{j \in S_p \setminus \{i\}} A_{i,j} \\ &= -\beta + 2 \sum_{j \in S_m \setminus \{i\}} A_{i,j} - 2|S_m|\beta + 2\beta \mathbf{1}_{[i \in S_m]} - 2\alpha \sum_{p \in [k] \setminus \{m\}} \sum_{j \in S_p \setminus \{i\}} A_{i,j}. \end{aligned} \quad (43)$$

In the last equality we use $-2 \sum_{j \in S_m \setminus \{i\}} \beta = -2|S_m|\beta + 2\beta \mathbf{1}_{[i \in S_m]}$. We note that computing the final expression in Eq. 43 is $O(k^2n)$, due to the last term. However, by noting that $\sum_{p \in [k] \setminus \{m\}} \sum_{j \in S_p \setminus \{i\}} A_{i,j} = \sum_{j \notin S_0} A_{i,j} - \sum_{j \in S_m \setminus \{i\}} A_{i,j}$ we can derive the following.

$$\begin{aligned}
 c_{im} &= -\beta + 2 \sum_{j \in S_m \setminus \{i\}} A_{i,j} - 2|S_m|\beta + 2\beta \mathbf{1}_{[i \in S_m]} - 2\alpha \sum_{p \in [k] \setminus \{m\}} \sum_{j \in S_p \setminus \{i\}} A_{i,j} \\
 &= -\beta + 2 \sum_{j \in S_m \setminus \{i\}} A_{i,j} - 2|S_m|\beta + 2\beta \mathbf{1}_{[i \in S_m]} - 2\alpha \left(\sum_{j \notin S_0} A_{i,j} - \sum_{j \in S_m \setminus \{i\}} A_{i,j} \right) \\
 &= -\beta + 2 \sum_{j \in S_m \setminus \{i\}} (A_{i,j} + \alpha A_{i,j}) - 2|S_m|\beta + 2\beta \mathbf{1}_{[i \in S_m]} - 2\alpha \sum_{j \notin S_0} A_{i,j} \\
 &= -\beta + 2(1 + \alpha) \sum_{j \in S_m \setminus \{i\}} A_{i,j} - 2|S_m|\beta + 2\beta \mathbf{1}_{[i \in S_m]} - 2\alpha \sum_{j \notin S_0} A_{i,j}
 \end{aligned} \tag{44}$$

Now, recall the definitions $M_{i,m} \triangleq 2 \sum_{j \in S_m} A_{i,j}$, $\eta_i \triangleq \sum_{m \in [k]} M_{i,m}$ and $\beta_{im} = 2\beta|S_m| - 2\beta \mathbf{1}_{[i \in S_m]}$. Then, we note that $2 \sum_{j \notin S_0} A_{i,j} = \sum_{m \in [k]} M_{i,m}$ (sum of all similarities from object i to all non-neutral objects). Then, we obtain the final expression, i.e.,

$$c_{im} = -\beta + (1 + \alpha)M_{i,m} - \beta_{im} - \alpha\eta_i, \quad \text{for } m \in [k], \tag{45}$$

The expression in Eq. 45 can be computed in $O(kn)$ since it just amounts to computing $M_{i,m}$ for all $m \in [k]$ (i.e., the total similarity from i to all non-neutral clusters $m \in [k]$).

□

Proposition 4. (a) There exists a $\xi_1 < 0$ such that for any $\beta \leq \xi_1$, there is a clustering solution maximizing Eq. 7 where all the objects are assigned to a single non-neutral cluster. (b) Conversely, there exists a $\xi_2 > 0$ such that for any $\beta \geq \xi_2$, there is a clustering solution maximizing Eq. 7 where all the objects are neutral.

Proof. By examining the gradient in Eq. 45, we observe that the dominant term involving β is $-\beta|S_m|$. Consequently, making β large and negative *increases* the incentive to assign objects to non-neutral clusters. Moreover, since $-\beta|S_m|$ scales with cluster size, the local search procedure will favor placing an object i in the largest non-neutral cluster. If β is sufficiently large and negative, this term will completely dominate the objective, ensuring that no object is assigned to the neutral set (as the contribution to all non-neutral clusters remains positive). Ultimately, all objects will be placed in the largest non-neutral cluster.

Similarly, if β is made very large and positive, $-\beta|S_m|$ will eventually dominate the objective, making the contribution to every non-neutral cluster negative for all objects. As a result, all objects will be assigned to the neutral set. □

B Experiments: More Details and Further Results

B.1 Datasets

Following (Tzeng et al., 2020), we consider the following widely studied real-world signed networks. **WoW-EP8** (W8) (Kristof et al., 2020) represents interactions among authors in the 8th EU Parliament legislature, where edge signs indicate collaboration or competition. **Bitcoin** (BTC) (Leskovec and Krevl, 2014) is a trust-distrust network of users trading on the Bitcoin OTC platform. **WikiVot** (WikiV) (Leskovec and Krevl, 2014) records positive and negative votes for Wikipedia admin elections. **Referendum** (REF) (Lai et al., 2018) captures tweets about the 2016 Italian constitutional referendum, with edge signs indicating whether users share the same stance. **Slashdot** (SD) (Leskovec and Krevl, 2014) is a friend-foe network from the Slashdot Zoo feature. **WikiCon** (WikiC) (Kunegis, 2013) tracks positive and negative interactions between users editing English Wikipedia. **Epinions** (EP) (Leskovec and Krevl, 2014) represents the trust-distrust relationships in the Epinions online social network. **WikiPol** (WikiP) (Maniu et al., 2011) captures interactions among users editing Wikipedia pages on political topics.

B.2 Baselines

For SCG, we use the public implementation from (Ruo-Chun Tzeng, 2020). For KOCG, we use the public implementation from (Lingyang Chu, 2016) with default hyperparameters: $\alpha = 1/(k-1)$, $\beta = 50$ (note that the purpose of this β differs from the one used in our paper), and $\ell = 5000$. For the spectral methods SPONGE and BNC, we use the public implementations from (Peter Davies and Aldo Glielmo, 2019). Following (Tzeng et al., 2020), for SPONGE, we evaluate both the *unnormalized* and *symmetric normalized* versions and report results for the best-performing method.

B.3 Complete Results on All Datasets

Tables 4-5 report results for polarity and BA-Polarity with $k = 2$, $k = 4$, and $k = 6$. The conclusions for $k = 2$ are consistent with those for $k = 4$ and $k = 6$, discussed in the main paper. According to these results, our method consistently achieves the highest scores or performs competitively with the best scores.

Tables 6-13 present detailed analyses for all datasets across 12 different aspects, including polarity and BA-polarity. They provide insights into the differences between the clustering solutions computed by each method. In the context of PCD, evaluating clustering quality is inherently subjective, as different aspects capture different aspects of the solution. Generally, there is a trade-off among these aspects, and the objective is to achieve a good balance between them. Below, we define the aspects used in our analysis. We have defined these aspects such that a larger number is better (apart from runtime).

Let $N = \sum_{m \in [k]} |S_m|$ denote the number of non-neutral objects, and let $N_{\text{nz}} = N_{\text{intra}}^+ + N_{\text{intra}}^- + N_{\text{inter}}^- + N_{\text{inter}}^+$ represent the number of non-zero similarities between non-neutral objects.

- **SIZE** = N : The total number of non-neutral objects.
- **BAL** = S_m/S_l : The balance factor, where S_m and S_l are the largest and smallest non-neutral clusters, respectively. Its range is $[0, 1]$, with 1 indicating perfect balance.
- **K**: The number of non-empty non-neutral clusters.
- **MAC**: *Mean Average Cohesion*, quantifying the density of positive intra-cluster similarities, defined as

$$\text{MAC} = \frac{1}{k} \sum_{m \in [k]} \frac{1}{|S_m|(|S_m| - 1)} \sum_{i,j \in S_m} A_{i,j}^+.$$

Its range is $[0, 1]$, where higher values indicate stronger cohesion within clusters.

- **MAO**: *Mean Average Opposition*, measuring the density of negative inter-cluster similarities, defined as

$$\text{MAO} = \frac{1}{k(k-1)} \sum_{\substack{m \in [k] \\ p \in [k] \setminus \{m\}}} \frac{1}{|S_m||S_p|} \sum_{\substack{i \in S_m \\ j \in S_p}} A_{i,j}^-.$$

Its range is $[0, 1]$, where higher values indicate stronger opposition between clusters.

- **CC+**: Measures the fraction of intra-cluster similarities that are positive minus those that are negative, defined as

$$\text{CC+} = \frac{N_{\text{intra}}^+ - N_{\text{intra}}^-}{N_{\text{intra}}^+ + N_{\text{intra}}^-}.$$

Its range is $[-1, 1]$, where -1 indicates that all non-zero intra-cluster similarities are negative, and $+1$ indicates that all are positive.

- **CC-**: Measures the fraction of inter-cluster similarities that are negative minus those that are positive, defined as

$$\text{CC-} = \frac{N_{\text{inter}}^- - N_{\text{inter}}^+}{N_{\text{inter}}^- + N_{\text{inter}}^+}.$$

Its range is $[-1, 1]$, where -1 indicates that all non-zero inter-cluster similarities are positive, and $+1$ indicates that all are negative.

- **DENS**: The proportion of non-zero similarities among non-neutral objects, defined as

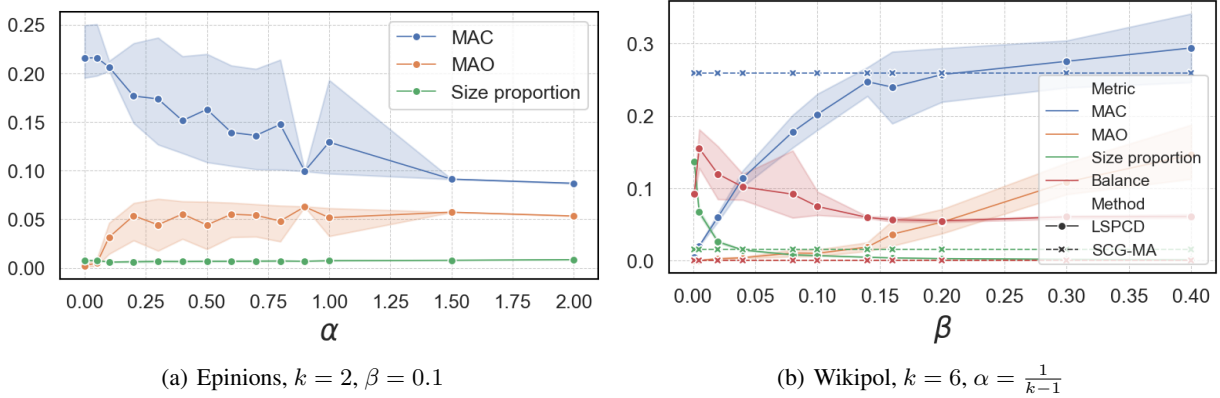
$$\text{DENS} = \frac{N_{\text{nz}}}{N(N-1)}.$$

Its range is $[0, 1]$, with higher values indicating denser connectivity.

- **ISO**: *Isolation*, measuring the separation between non-neutral and neutral objects, defined as

$$\text{ISO} = \frac{N_{\text{nz}}}{N_{\text{nz}} + \sum_{i \in S_0} \sum_{j \notin S_0} |A_{i,j}|}.$$

Its range is $[0, 1]$, where $\text{ISO} = 1$ means non-neutral objects are fully isolated from neutral ones, meaning no non-zero edges exist between them (which is ideal).


 Figure 2: Investigation of the impact of α and β .

- POL: *Polarity*, as defined in the main paper.
- BA-POL: *Balance-aware polarity*, as defined in the main paper.
- RT: Runtime of the corresponding method in seconds.

From Tables 6-13, we derive several key insights. Firstly, our method exhibits low standard deviation, indicating robustness to the initial random solution. It consistently finds high-polarity solutions while maintaining better balance than its main competitor, SCG. Unlike some baselines such as KOCG and SPONGE, our method does not enforce excessive balance, ensuring solutions remain both high in polarity and reasonably balanced.

In terms of runtime, our method is efficient and competitive with the baselines. It is also consistently ranked among the best in both DENS and ISO. Unlike SCG, our method always identifies k non-empty non-neutral clusters, which we argue is a significant limitation of SCG.

While SCG generally achieves higher MAC values, this is largely due to its tendency to produce highly imbalanced solutions, often with singleton clusters. Since small or singleton clusters trivially yield high average cohesion (values close to 1), they can disproportionately inflate the overall MAC score.

Finally, our method performs comparably or better than SCG in CC+ and significantly outperforms it in CC- in most cases. This highlights another limitation of SCG: it often includes more positive similarities between clusters than negative ones, as reflected by negative CC- values. Some baselines produce either overly large or overly small non-neutral clusters (based on SIZE), whereas our method consistently finds solutions with a reasonable number of non-neutral objects (which consequently leads to a good balance of the other aspects), similar to SCG. However, we note that we can easily adjust the number of non-neutral objects by adjusting β , as discussed in the paper.

In Figure 2, we illustrate the impact of varying α and β . According to Figure 2(a), increasing α naturally balances intra-cluster cohesion and inter-cluster opposition. The size proportion, defined as the fraction of non-neutral objects in V , remains constant as α varies. Figure 2(b) shows that increasing β monotonically reduces the number of non-neutral objects, leading to denser clusters, as indicated by improved MAC and MAO scores. Notably, balance remains stable across different β values, unlike the baseline SCG-MA.

C Limitations of Polarity

To illustrate the limitation of polarity, we refer to Example 2 from (Gullo et al., 2024), which considers a signed graph with 12 objects: $\{A, B, C, D, E, F, G, H, I, J, K, L\}$. The sign of each similarity can be found in Figure 3 of (Gullo et al., 2024). The study evaluates the following three clustering solutions:

- $S^{(1)} = \{\{A, B, C, D\}, \{E, F, G, H\}\}$
- $S^{(2)} = \{\{A, B, C, D\}, \{E, F, G, H, I, J, K, L\}\}$
- $S^{(3)} = \{\emptyset, \{E, F, G, H, I, J, K, L\}\}$

Table 4: Results for different methods and datasets w.r.t. the *balance-aware polarity* metric. $|E|$ is the number of non-zero edges and $|E_-|$ is the number of negative edges. We observe that our method (LSPCD) often yields the highest scores.

		W8	BTC	WIKI V	REF	SD	WIKI C	EP	WIKI P
	$ V $	790	5.9K	7.1K	10.9K	82.1K	116.7K	131.6K	138.6K
	$ E $	116K	214.5K	1M	251.4K	500.5K	2M	711.2K	715.9K
	$ E_- / E $	0.2	0.2	0.2	0.1	0.2	0.6	0.2	0.1
$k = 2$	LSPCD (OURS)	19.4	10.9	13.9	61.8	9.7	102.2	56.2	12.4
	SCG-MA	0.4	2.4	0.4	1.3	0.8	44.7	2.5	0.6
	SCG-MO	0.5	0.6	0.4	1.3	0.7	39.6	2.4	0.4
	SCG-B	4.9	19.7	0.7	1.7	1.5	47.3	3.8	0.9
	SCG-R	3.4	1.8	4.6	2.1	1.1	31.9	6.6	3.0
	KOCCG-TOP-1	10.4	1.0	3.8	4.8	1.3	3.5	3.3	1.8
	KOCCG-TOP- r	11.3	3.3	2.2	11.7	2.2	2.9	10.1	1.1
	BNC- $(k+1)$	-0.4	-0.9	-0.6	-1.0	—	—	—	—
	BNC- k	0.7	0.0	0.0	0.0	—	—	—	—
	SPONGE- $(k+1)$	19.7	0.6	0.3	0.6	—	—	—	—
	SPONGE- k	22.4	0.0	0.0	0.0	—	—	—	—
$k = 4$	LSPCD (OURS)	6.9	3.6	5.9	3.9	6.7	26.3	14.9	5.4
	SCG-MA	5.8	0.3	0.8	0.3	1.9	0.7	0.1	0.7
	SCG-MO	4.9	0.3	0.4	0.4	0.2	6.6	0.1	0.0
	SCG-B	0.3	0.1	0.2	0.1	0.5	18.5	0.2	0.1
	SCG-R	1.3	0.9	0.9	0.6	2.4	2.0	0.3	1.0
	KOCCG-TOP-1	5.8	4.2	1.2	2.6	0.9	0.4	4.0	0.9
	KOCCG-TOP- r	5.4	2.7	2.6	1.6	1.0	2.8	5.9	1.2
	BNC- $(k+1)$	-0.1	-0.8	-0.4	-1.0	—	—	—	—
	BNC- k	0.5	0.0	0.0	0.0	—	—	—	—
	SPONGE- $(k+1)$	22.9	0.0	0.4	0.3	—	—	—	—
	SPONGE- k	18.6	0.0	0.0	0.0	—	—	—	—
$k = 6$	LSPCD (OURS)	4.4	2.2	3.6	2.2	3.8	16.4	6.8	3.5
	SCG-MA	3.1	0.1	0.2	0.1	0.0	0.6	0.4	0.0
	SCG-MO	3.6	0.1	0.2	0.1	0.1	4.2	0.1	0.0
	SCG-B	0.3	0.2	0.2	0.1	0.2	1.8	0.2	0.1
	SCG-R	0.3	0.3	0.4	0.2	0.4	2.3	0.1	0.0
	KOCCG-TOP-1	6.1	1.7	2.5	3.3	1.7	0.4	2.7	3.7
	KOCCG-TOP- r	5.0	1.2	1.8	2.5	1.3	1.1	2.8	0.7
	BNC- $(k+1)$	-0.1	-0.1	-0.8	-0.4	—	—	—	—
	BNC- k	0.5	0.0	0.0	0.0	—	—	—	—
	SPONGE- $(k+1)$	17.7	0.0	0.4	0.6	—	—	—	—
	SPONGE- k	16.0	0.0	0.0	0.0	—	—	—	—

The polarity values for these solutions are: $\text{Polarity}(S^{(1)}) = (20+10)/8 = 3.75$, $\text{Polarity}(S^{(2)}) = (38+6)/12 = 3.67$, and $\text{Polarity}(S^{(3)}) = (30+0)/8 = 3.75$.

Although $S^{(1)}$ and $S^{(3)}$ achieve the same polarity score, $S^{(1)}$ is significantly more balanced, making it the more reasonable choice. In contrast, evaluating our objective (Eq. 7) for the same solutions, we obtain $S^{(1)} : (20+10) - (4^2+4^2) = -2$, $S^{(2)} : (38+6) - (4^2+8^2) = -36$, and $S^{(3)} : (30+0) - 8^2 = -34$.

Our objective function still identifies $S^{(2)}$ as the worst solution (consistent with polarity), but it strongly favors $S^{(1)}$ over $S^{(3)}$ due to its better balance. Here, we assume $\alpha = 1/(k-1)$ (which is 1 since $k=2$) for consistency with polarity, and $\beta = 1$.

Table 5: Results for different methods and datasets w.r.t. the *polarity* metric. $|E|$ is the number of non-zero edges and $|E_-|$ is the number of negative edges. Our method (LSPCD) yields the best or competitive results, despite the fact that it, unlike SCG methods, does not directly optimize polarity.

		W8	BTC	WIKIV	REF	SD	WIKIC	EP	WIKIP
	$ V $	790	5.9K	7.1K	10.9K	82.1K	116.7K	131.6K	138.6K
	$ E $	116K	214.5K	1M	251.4K	500.5K	2M	711.2K	715.9K
	$ E_- / E $	0.2	0.2	0.2	0.1	0.2	0.6	0.2	0.1
$k = 2$	LSPCD (OURS)	223.4	29.0	62.3	146.1	75.9	190.8	127.8	82.0
	SCG-MA	236.6	28.8	71.5	172.2	77.5	155.2	128.3	82.8
	SCG-MO	236.6	29.5	71.7	174.1	79.7	175.7	128.7	88.4
	SCG-B	200.6	21.6	37.6	116.3	61.0	129.3	156.4	46.5
	SCG-R	214.6	14.2	54.7	120.9	29.7	101.1	72.3	36.1
	KOCCG-TOP-1	13.0	1.0	7.6	11.6	2.0	5.9	8.2	3.0
	KOCCG-TOP- r	13.0	3.8	2.3	15.4	2.6	3.4	14.0	1.3
	BNC- $(k + 1)$	-0.7	-10.8	-1.1	-1.0	—	—	—	—
	BNC- k	184.6	5.3	15.8	41.5	—	—	—	—
	SPONGE- $(k + 1)$	88.0	1.0	1.0	1.0	—	—	—	—
SPONGE- k	191.4	5.1	15.8	41.5	—	—	—	—	
$k = 4$	LSPCD (OURS)	218.5	23.3	52.6	139.2	61.1	113.6	111.5	71.6
	SCG-MA	205.1	25.1	52.9	94.5	35.5	104.9	127.4	56.5
	SCG-MO	213.2	25.3	53.1	82.1	38.5	117.9	129.0	39.7
	SCG-B	211.6	12.4	24.8	116.2	48.3	49.8	94.4	45.7
	SCG-R	214.6	8.0	19.5	118.7	10.7	41.1	65.1	33.7
	KOCCG-TOP-1	9.1	8.4	4.5	15.0	2.6	4.5	8.9	3.1
	KOCCG-TOP- r	7.4	5.0	3.3	3.7	3.0	3.8	11.0	4.4
	BNC- $(k + 1)$	-0.2	-9.4	-1.1	-1.0	—	—	—	—
	BNC- k	185.3	5.2	15.8	41.5	—	—	—	—
	SPONGE- $(k + 1)$	53.8	1.1	1.0	1.0	—	—	—	—
SPONGE- k	71.2	5.1	15.8	41.5	—	—	—	—	
$k = 6$	LSPCD (OURS)	217.3	20.0	46.2	137.6	57.1	96.1	103.4	58.7
	SCG-MA	207.3	14.6	45.5	84.9	37.8	102.6	88.8	57.5
	SCG-MO	205.8	15.2	47.0	55.6	34.6	111.6	129.2	41.8
	SCG-B	211.6	9.3	23.3	116.2	47.7	46.1	94.5	46.0
	SCG-R	201.2	6.9	10.4	50.3	7.9	18.3	43.3	3.3
	KOCCG-TOP-1	7.9	4.1	4.5	8.6	3.6	4.9	6.0	10.1
	KOCCG-TOP- r	9.1	3.6	3.1	4.0	3.3	1.5	6.8	3.6
	BNC- $(k + 1)$	-0.2	-4.2	-1.1	-0.8	—	—	—	—
	BNC- k	185.2	5.2	15.8	41.5	—	—	—	—
	SPONGE- $(k + 1)$	47.8	1.3	1.0	1.0	—	—	—	—
SPONGE- k	57.9	5.1	15.8	41.5	—	—	—	—	

Table 6: Detailed results on the **WoW-EP8** dataset from various aspects. LSPCD (avg) and LSPCD (std) respectively indicate the mean and standard deviation across five runs of our method with different seeds.

		SIZE	BAL	K	MAC	MAO	CC+	CC-	DENS	ISO	POL	BA-POL	RT
$k = 2$	LSPCD (AVG)	586	0.087	2	0.261	0.098	0.757	0.509	0.511	0.769	223.406	19.409	0.249
	LSPCD (STD)	0	0.0	0	0.0	0.0	0.0	0.0	0.0	0.0	0.0	0.0	0.034
	SCG-MA	527	0.002	1	0.52	0.0	0.762	0.0	0.59	0.725	236.55	0.448	1.025
	SCG-MO	517	0.002	1	0.527	0.0	0.769	0.0	0.596	0.708	236.592	0.457	1.026
	SCG-B	583	0.025	2	0.274	0.094	0.697	-0.369	0.514	0.767	200.604	4.918	4.657
	SCG-R	513	0.016	2	0.272	0.104	0.761	0.451	0.552	0.654	214.616	3.386	0.517
	KOCCG-TOP-1	16	0.8	2	0.986	0.889	0.965	0.778	1.0	0.019	13.0	10.4	—
	KOCCG-TOP- r	527	0.869	2	0.467	0.11	0.658	-0.598	0.559	0.691	12.964	11.269	—
	BNC- $(k + 1)$	3	0.667	2	0.5	0.0	-1.0	0.0	0.333	0.007	-0.667	-0.444	0.99
	BNC- k	790	0.004	2	0.152	0.049	0.628	1.0	0.372	1.0	184.63	0.702	0.537
	SPONGE- $(k + 1)$	375	0.224	2	0.204	0.095	0.738	0.318	0.343	0.346	87.957	19.705	0.581
	SPONGE- k	790	0.117	2	0.191	0.093	0.696	0.15	0.372	1.0	191.38	22.404	0.572
$k = 4$	LSPCD (AVG)	590	0.031	4	0.156	0.082	0.76	0.426	0.506	0.772	218.458	6.862	0.317
	LSPCD (STD)	1	0.0	0	0.003	0.002	0.001	0.016	0.0	0.002	0.142	0.008	0.044
	SCG-MA	599	0.028	4	0.58	0.13	0.762	-0.32	0.527	0.822	205.137	5.828	1.198
	SCG-MO	568	0.023	4	0.827	0.141	0.77	-0.349	0.55	0.776	213.211	4.939	1.176
	SCG-B	615	0.002	1	0.421	0.0	0.693	0.0	0.498	0.822	211.561	0.343	6.233
	SCG-R	503	0.006	4	0.211	0.056	0.762	0.747	0.564	0.644	214.623	1.301	1.131
	KOCCG-TOP-1	31	0.636	4	0.962	0.668	0.944	0.339	0.978	0.039	9.054	5.761	—
	KOCCG-TOP- r	599	0.735	4	0.436	0.099	0.692	-0.618	0.516	0.806	7.393	5.434	—
	BNC- $(k + 1)$	8	0.4	4	0.5	0.0	-1.0	0.0	0.036	0.003	-0.25	-0.1	0.62
	BNC- k	790	0.003	4	0.327	0.03	0.632	1.0	0.372	1.0	185.305	0.473	0.594
	SPONGE- $(k + 1)$	485	0.426	4	0.448	0.06	0.886	-0.53	0.33	0.433	53.823	22.911	0.593
	SPONGE- k	790	0.261	4	0.383	0.08	0.803	-0.499	0.372	1.0	71.162	18.585	0.61
$k = 6$	LSPCD (AVG)	591	0.02	6	0.142	0.071	0.761	0.414	0.505	0.773	217.344	4.419	0.269
	LSPCD (STD)	0	0.0	0	0.006	0.002	0.0	0.009	0.0	0.001	0.142	0.003	0.015
	SCG-MA	598	0.015	6	0.785	0.113	0.763	-0.339	0.527	0.819	207.299	3.141	1.226
	SCG-MO	591	0.017	6	0.756	0.171	0.77	-0.321	0.534	0.811	205.796	3.576	1.378
	SCG-B	615	0.002	1	0.421	0.0	0.693	0.0	0.498	0.822	211.561	0.343	7.512
	SCG-R	744	0.001	5	0.323	0.178	0.669	0.313	0.41	0.978	201.172	0.275	1.295
	KOCCG-TOP-1	42	0.778	6	0.992	0.605	0.984	0.303	0.934	0.053	7.905	6.148	—
	KOCCG-TOP- r	598	0.554	6	0.472	0.095	0.73	-0.637	0.522	0.812	9.109	5.045	—
	BNC- $(k + 1)$	10	0.5	6	0.5	0.0	-1.0	0.0	0.022	0.002	-0.2	-0.1	0.977
	BNC- k	790	0.003	6	0.552	0.016	0.632	1.0	0.372	1.0	185.198	0.473	0.61
	SPONGE- $(k + 1)$	572	0.372	6	0.537	0.065	0.893	-0.511	0.326	0.536	47.762	17.749	0.607
	SPONGE- k	790	0.276	6	0.53	0.075	0.834	-0.529	0.372	1.0	57.868	15.99	0.599

Table 7: Detailed results on the **Bitcoin** dataset from various aspects. LSPCD (avg) and LSPCD (std) respectively indicate the mean and standard deviation across five runs of our method with different seeds.

		SIZE	BAL	K	MAC	MAO	CC+	CC-	DENS	ISO	POL	BA-POL	RT
$k = 2$	LSPCD (AVG)	155	0.377	2	0.2	0.143	0.94	0.969	0.199	0.211	29.022	10.947	2.203
	LSPCD (STD)	0	0.0	0	0.0	0.0	0.003	0.001	0.001	0.001	0.013	0.005	0.161
	SCG-MA	179	0.084	2	0.298	0.068	0.906	0.873	0.179	0.216	28.838	2.418	0.122
	SCG-MO	138	0.022	2	0.114	0.147	0.91	0.778	0.237	0.184	29.522	0.646	0.123
	SCG-B	40	0.909	2	0.248	0.87	0.956	1.0	0.56	0.201	21.65	19.682	2.243
	SCG-R	842	0.124	2	0.022	0.009	0.908	0.812	0.019	0.394	14.24	1.763	1.024
	KOCCG-TOP-1	2	1.0	2	1.0	1.0	0.0	1.0	1.0	0.004	1.0	1.0	—
	KOCCG-TOP- r	179	0.885	2	0.063	0.055	0.266	0.182	0.094	0.165	3.754	3.324	—
	BNC- $(k + 1)$	50	0.083	2	0.058	0.0	-0.516	0.0	0.425	0.581	-10.76	-0.897	0.341
	BNC- k	5881	0.008	2	0.059	0.001	0.721	0.694	0.001	1.0	5.268	0.043	0.202
	SPONGE- $(k + 1)$	6	0.6	2	0.667	0.0	1.0	0.0	0.2	1.0	1.0	0.6	1.116
	SPONGE- k	5881	0.001	2	0.501	0.0	0.697	0.0	0.001	1.0	5.092	0.003	2.138
$k = 4$	LSPCD (AVG)	217	0.154	4	0.182	0.12	0.929	0.815	0.143	0.256	23.333	3.586	2.117
	LSPCD (STD)	13	0.028	0	0.027	0.029	0.004	0.123	0.011	0.009	0.765	0.534	0.408
	SCG-MA	176	0.014	4	0.488	0.07	0.914	-0.44	0.172	0.2	25.121	0.349	0.302
	SCG-MO	180	0.014	4	0.487	0.07	0.91	-0.431	0.169	0.205	25.252	0.341	0.348
	SCG-B	216	0.011	4	0.473	0.052	0.865	0.296	0.076	0.176	12.401	0.142	6.377
	SCG-R	450	0.11	4	0.036	0.008	0.92	-0.627	0.033	0.238	8.033	0.886	1.237
	KOCCG-TOP-1	26	0.5	4	0.859	0.621	1.0	0.653	0.738	0.112	8.41	4.205	—
	KOCCG-TOP- r	176	0.54	4	0.136	0.041	0.856	-0.246	0.113	0.157	5.034	2.717	—
	BNC- $(k + 1)$	58	0.083	4	0.112	0.0	-0.516	0.0	0.32	0.576	-9.414	-0.784	0.185
	BNC- k	5881	0.001	4	0.029	0.0	0.721	0.67	0.001	1.0	5.208	0.004	0.178
	SPONGE- $(k + 1)$	71	0.045	4	0.754	0.0	1.0	0.0	0.016	0.443	1.099	0.05	3.364
	SPONGE- k	5881	0.001	4	0.75	0.0	0.697	0.0	0.001	1.0	5.092	0.003	2.797
$k = 6$	LSPCD (AVG)	194	0.114	6	0.251	0.143	0.948	0.646	0.155	0.231	20.031	2.201	2.73
	LSPCD (STD)	23	0.044	0	0.046	0.053	0.007	0.304	0.019	0.015	1.827	0.582	0.468
	SCG-MA	430	0.009	6	0.536	0.021	0.931	-0.355	0.055	0.301	14.568	0.125	0.448
	SCG-MO	412	0.009	6	0.571	0.028	0.929	-0.337	0.058	0.3	15.165	0.14	0.477
	SCG-B	326	0.017	6	0.313	0.009	0.866	-0.421	0.053	0.222	9.321	0.16	10.509
	SCG-R	860	0.038	6	0.038	0.006	0.941	-0.529	0.017	0.367	6.861	0.258	2.125
	KOCCG-TOP-1	28	0.429	6	0.867	0.338	1.0	0.197	0.537	0.055	4.071	1.745	—
	KOCCG-TOP- r	430	0.333	6	0.077	0.013	0.88	-0.405	0.043	0.26	3.601	1.2	—
	BNC- $(k + 1)$	224	0.018	6	0.075	0.001	-0.622	0.958	0.033	0.394	-4.239	-0.077	0.286
	BNC- k	5881	0.001	6	0.075	0.0	0.722	0.657	0.001	1.0	5.197	0.003	0.194
	SPONGE- $(k + 1)$	222	0.016	6	0.622	0.0	1.0	0.0	0.006	0.401	1.252	0.02	1.959
	SPONGE- k	5881	0.001	6	0.563	0.0	0.696	-1.0	0.001	1.0	5.085	0.003	2.473

Table 8: Detailed results on the **WikiVot** dataset from various aspects. LSPCD (avg) and LSPCD (std) respectively indicate the mean and standard deviation across five runs of our method with different seeds.

		SIZE	BAL	K	MAC	MAO	CC+	CC-	DENS	ISO	POL	BA-POL	RT
$k = 2$	LSPCD (AVG)	1278	0.224	2	0.038	0.015	0.831	0.673	0.06	0.548	62.322	13.948	2.457
	LSPCD (STD)	4	0.001	0	0.0	0.0	0.0	0.003	0.0	0.001	0.003	0.056	0.276
	SCG-MA	813	0.005	2	0.048	0.079	0.846	0.671	0.104	0.436	71.476	0.353	1.537
	SCG-MO	748	0.005	2	0.052	0.082	0.854	0.671	0.113	0.411	71.733	0.385	1.432
	SCG-B	414	0.02	2	0.054	0.033	0.756	0.776	0.12	0.221	37.589	0.737	7.501
	SCG-R	1100	0.085	2	0.032	0.013	0.83	0.618	0.061	0.444	54.693	4.63	0.781
	KOCCG-TOP-1	10	0.5	2	0.905	0.857	1.0	1.0	0.844	0.012	7.6	3.8	—
	KOCCG-TOP- r	813	0.964	2	0.047	0.022	0.427	-0.337	0.066	0.297	2.312	2.229	—
	BNC- $(k + 1)$	9	0.571	2	0.0	0.0	-1.0	0.0	0.139	1.0	-1.111	-0.635	0.721
	BNC- k	7115	0.002	2	0.002	0.0	0.558	0.0	0.004	1.0	15.794	0.024	0.49
	SPONGE- $(k + 1)$	10	0.333	2	0.571	0.0	1.0	0.0	0.111	1.0	1.0	0.333	1.602
	SPONGE- k	7115	0.002	2	0.057	0.0	0.558	0.0	0.004	1.0	15.794	0.024	0.977
$k = 4$	LSPCD (AVG)	1089	0.115	4	0.073	0.013	0.856	-0.045	0.072	0.489	52.605	5.869	4.381
	LSPCD (STD)	149	0.029	0	0.026	0.002	0.004	0.427	0.011	0.04	6.003	0.86	1.69
	SCG-MA	1142	0.015	4	0.081	0.018	0.849	-0.618	0.069	0.506	52.945	0.78	2.042
	SCG-MO	1059	0.007	4	0.089	0.022	0.858	-0.692	0.073	0.474	53.07	0.356	1.986
	SCG-B	790	0.01	4	0.091	0.014	0.774	-0.718	0.077	0.342	24.782	0.243	18.286
	SCG-R	1524	0.044	4	0.031	0.008	0.813	-0.68	0.043	0.549	19.524	0.861	3.074
	KOCCG-TOP-1	33	0.267	4	0.845	0.086	0.933	-0.609	0.576	0.03	4.525	1.207	—
	KOCCG-TOP- r	1142	0.803	4	0.055	0.011	0.719	-0.618	0.059	0.44	3.288	2.639	—
	BNC- $(k + 1)$	15	0.333	4	0.0	0.0	-1.0	0.0	0.076	1.0	-1.067	-0.356	0.527
	BNC- k	7115	0.0	4	0.001	0.0	0.558	0.0	0.004	1.0	15.794	0.007	0.533
	SPONGE- $(k + 1)$	12	0.429	4	0.8	0.0	1.0	0.0	0.091	1.0	1.0	0.429	2.327
	SPONGE- k	7115	0.001	4	0.156	0.0	0.558	0.0	0.004	1.0	15.794	0.011	1.522
$k = 6$	LSPCD (AVG)	534	0.078	6	0.143	0.029	0.896	-0.314	0.133	0.287	46.179	3.586	5.292
	LSPCD (STD)	46	0.008	0	0.015	0.002	0.004	0.07	0.012	0.008	2.177	0.201	0.931
	SCG-MA	1355	0.004	6	0.064	0.023	0.849	-0.647	0.056	0.564	45.494	0.168	2.24
	SCG-MO	1226	0.004	6	0.073	0.024	0.859	-0.683	0.063	0.526	47.013	0.189	2.178
	SCG-B	941	0.01	6	0.121	0.018	0.78	-0.735	0.065	0.369	23.332	0.229	29.072
	SCG-R	1501	0.043	6	0.039	0.008	0.817	-0.734	0.044	0.542	10.433	0.444	3.475
	KOCCG-TOP-1	40	0.556	6	0.894	0.227	0.981	-0.188	0.564	0.033	4.52	2.511	—
	KOCCG-TOP- r	1355	0.561	6	0.051	0.009	0.73	-0.62	0.05	0.506	3.132	1.757	—
	BNC- $(k + 1)$	13	0.75	6	0.0	0.0	-1.0	0.0	0.09	1.0	-1.077	-0.808	0.966
	BNC- k	7115	0.0	6	0.001	0.0	0.558	0.0	0.004	1.0	15.794	0.007	0.546
	SPONGE- $(k + 1)$	20	0.429	6	0.644	0.0	1.0	0.0	0.053	1.0	1.0	0.429	1.791
	SPONGE- k	7115	0.0	6	0.434	0.0	0.558	0.0	0.004	1.0	15.794	0.007	1.66

Table 9: Detailed results on the **Referendum** dataset from various aspects. LSPCD (avg) and LSPCD (std) respectively indicate the mean and standard deviation across five runs of our method with different seeds.

		SIZE	BAL	K	MAC	MAO	CC+	CC-	DENS	ISO	POL	BA-POL	RT
$k = 2$	LSPCD (AVG)	915	0.423	2	0.279	0.014	1.0	0.114	0.17	0.353	146.109	61.846	3.376
	LSPCD (STD)	1	0.002	0	0.001	0.0	0.0	0.017	0.001	0.001	0.092	0.233	0.19
	SCG-MA	824	0.007	2	0.455	0.247	1.0	0.558	0.211	0.409	172.206	1.26	1.863
	SCG-MO	673	0.007	2	0.546	0.3	1.0	0.571	0.261	0.352	174.083	1.299	1.108
	SCG-B	1158	0.015	2	0.176	0.068	1.0	0.58	0.101	0.396	116.252	1.729	23.313
	SCG-R	1550	0.018	2	0.095	0.04	1.0	0.529	0.079	0.492	120.85	2.14	4.657
	KOCCG-TOP-1	15	0.417	2	0.973	0.659	1.0	1.0	0.829	0.007	11.6	4.833	—
	KOCCG-TOP- r	824	0.761	2	0.057	0.018	0.705	-0.317	0.065	0.169	15.425	11.741	—
	BNC- $(k + 1)$	4	1.0	2	0.0	0.0	-1.0	0.0	0.333	0.286	-1.0	-1.0	1.929
	BNC- k	10884	0.0	2	0.002	0.0	0.898	-1.0	0.004	1.0	41.495	0.011	1.114
	SPONGE- $(k + 1)$	6	0.6	2	0.667	0.0	1.0	0.0	0.2	1.0	1.0	0.6	6.754
	SPONGE- k	10884	0.0	2	0.502	0.0	0.898	0.0	0.004	1.0	41.495	0.011	6.889
$k = 4$	LSPCD (AVG)	1065	0.028	4	0.196	0.043	1.0	0.056	0.145	0.394	139.163	3.915	3.724
	LSPCD (STD)	1	0.0	0	0.0	0.0	0.0	0.001	0.0	0.0	0.037	0.006	0.392
	SCG-MA	1713	0.004	4	0.124	0.048	1.0	-0.693	0.081	0.512	94.544	0.348	6.809
	SCG-MO	1658	0.004	4	0.142	0.054	1.0	-0.767	0.084	0.502	82.139	0.355	3.863
	SCG-B	1142	0.001	1	0.102	0.0	1.0	0.0	0.102	0.398	116.233	0.102	60.02
	SCG-R	1514	0.005	4	0.174	0.019	1.0	0.432	0.08	0.479	118.706	0.559	2.545
	KOCCG-TOP-1	53	0.172	4	0.85	0.297	1.0	-0.363	0.615	0.024	14.956	2.579	—
	KOCCG-TOP- r	1713	0.426	4	0.065	0.003	0.885	-0.862	0.052	0.363	3.711	1.581	—
	BNC- $(k + 1)$	8	1.0	4	0.0	0.0	-1.0	0.0	0.143	0.25	-1.0	-1.0	1.125
	BNC- k	10884	0.0	4	0.001	0.0	0.898	-0.429	0.004	1.0	41.495	0.011	1.129
	SPONGE- $(k + 1)$	18	0.333	4	0.452	0.0	1.0	0.0	0.059	1.0	1.0	0.333	5.042
	SPONGE- k	10884	0.0	4	0.156	0.0	0.898	0.0	0.004	1.0	41.495	0.019	6.327
$k = 6$	LSPCD (AVG)	1021	0.016	6	0.176	0.028	1.0	0.04	0.15	0.379	137.627	2.211	5.461
	LSPCD (STD)	1	0.001	0	0.001	0.0	0.0	0.001	0.0	0.0	0.131	0.081	2.813
	SCG-MA	1945	0.001	5	0.107	0.033	1.0	-0.771	0.069	0.56	84.933	0.104	8.225
	SCG-MO	2469	0.001	5	0.16	0.003	1.0	-0.853	0.049	0.629	55.571	0.071	6.925
	SCG-B	1142	0.001	1	0.102	0.0	1.0	0.0	0.102	0.398	116.233	0.102	98.669
	SCG-R	1660	0.005	6	0.08	0.038	0.986	-0.756	0.052	0.356	50.258	0.247	5.075
	KOCCG-TOP-1	81	0.381	6	0.923	0.088	1.0	-0.673	0.536	0.032	8.622	3.285	—
	KOCCG-TOP- r	1945	0.63	6	0.061	0.003	0.917	-0.876	0.053	0.442	4.037	2.543	—
	BNC- $(k + 1)$	12	0.5	6	0.222	0.0	-0.714	0.0	0.106	0.25	-0.833	-0.417	1.923
	BNC- k	10884	0.0	6	0.056	0.0	0.898	-0.2	0.004	1.0	41.495	0.011	1.155
	SPONGE- $(k + 1)$	18	0.6	6	0.667	0.0	1.0	0.0	0.059	1.0	1.0	0.6	11.664
	SPONGE- k	10884	0.0	6	0.501	0.0	0.898	0.0	0.004	1.0	41.495	0.011	9.346

Table 10: Detailed results on the **Slashdot** dataset from various aspects. LSPCD (avg) and LSPCD (std) respectively indicate the mean and standard deviation across five runs of our method with different seeds.

		SIZE	BAL	K	MAC	MAO	CC+	CC-	DENS	ISO	POL	BA-POL	RT
$k = 2$	LSPCD (AVG)	235	0.128	2	0.207	0.055	0.969	0.836	0.337	0.167	75.903	9.686	29.957
	LSPCD (STD)	0	0.002	0	0.0	0.001	0.0	0.003	0.001	0.0	0.095	0.133	3.151
	SCG-MA	307	0.01	2	0.63	0.123	0.968	0.923	0.262	0.152	77.485	0.76	3.316
	SCG-MO	234	0.009	2	0.674	0.137	0.973	0.882	0.352	0.145	79.692	0.681	2.654
	SCG-B	289	0.025	2	0.145	0.056	0.98	-0.005	0.221	0.205	60.962	1.503	287.233
	SCG-R	3033	0.036	2	0.007	0.007	0.872	0.635	0.011	0.216	29.706	1.065	25.778
	KOCCG-TOP-1	3	0.667	2	1.0	1.0	1.0	1.0	1.0	0.005	2.0	1.333	—
	KOCCG-TOP- r	307	0.828	2	0.028	0.03	0.159	0.182	0.05	0.037	2.612	2.164	—
$k = 4$	LSPCD (AVG)	380	0.11	4	0.212	0.087	0.966	0.492	0.192	0.189	61.089	6.738	37.751
	LSPCD (STD)	2	0.005	0	0.01	0.003	0.0	0.004	0.002	0.001	0.251	0.261	3.013
	SCG-MA	2552	0.054	4	0.159	0.012	0.862	-0.431	0.026	0.269	35.53	1.907	16.032
	SCG-MO	2111	0.004	4	0.181	0.051	0.876	-0.657	0.03	0.24	38.534	0.153	21.868
	SCG-B	410	0.011	4	0.287	0.101	0.973	-0.491	0.128	0.199	48.306	0.51	814.654
	SCG-R	3853	0.223	4	0.01	0.002	0.877	-0.34	0.008	0.227	10.749	2.396	27.234
	KOCCG-TOP-1	23	0.364	4	0.453	0.172	1.0	0.643	0.206	0.009	2.609	0.949	—
	KOCCG-TOP- r	2552	0.34	4	0.013	0.003	0.627	-0.477	0.012	0.16	2.973	1.012	—
$k = 6$	LSPCD (AVG)	272	0.066	6	0.306	0.083	0.982	0.423	0.251	0.156	57.075	3.759	64.95
	LSPCD (STD)	30	0.009	0	0.041	0.013	0.001	0.134	0.032	0.014	2.428	0.393	24.494
	SCG-MA	2343	0.001	5	0.35	0.026	0.868	-0.701	0.028	0.256	37.849	0.02	32.081
	SCG-MO	2504	0.003	6	0.212	0.063	0.876	-0.421	0.026	0.265	34.649	0.098	26.278
	SCG-B	420	0.004	3	0.254	0.005	0.971	-0.481	0.124	0.191	47.676	0.168	1408.849
	SCG-R	9661	0.045	6	0.02	0.002	0.814	-0.43	0.004	0.433	7.906	0.359	73.943
	KOCCG-TOP-1	48	0.467	6	0.65	0.079	0.978	-0.166	0.216	0.016	3.583	1.672	—
	KOCCG-TOP- r	2343	0.408	6	0.021	0.003	0.722	-0.54	0.014	0.164	3.28	1.34	—

Table 11: Detailed results on the **WikiCon** dataset from various aspects. LSPCD (avg) and LSPCD (std) respectively indicate the mean and standard deviation across five runs of our method with different seeds.

		SIZE	BAL	K	MAC	MAO	CC+	CC-	DENS	ISO	POL	BA-POL	RT
$k = 2$	LSPCD (AVG)	1876	0.536	2	0.055	0.128	0.871	0.997	0.108	0.242	190.8	102.249	72.368
	LSPCD (STD)	0	0.0	0	0.0	0.0	0.0	0.0	0.0	0.0	0.019	0.066	17.051
	SCG-MA	8903	0.288	2	0.008	0.026	0.81	0.998	0.019	0.473	155.215	44.697	69.196
	SCG-MO	2442	0.226	2	0.036	0.094	0.839	0.999	0.08	0.22	175.654	39.641	19.316
	SCG-B	502	0.366	2	0.117	0.387	0.816	0.926	0.295	0.142	129.335	47.318	1314.819
	SCG-R	12669	0.316	2	0.004	0.011	0.798	0.997	0.009	0.441	101.138	31.924	169.997
	KOCCG-TOP-1	14	0.6	2	0.803	0.289	0.85	0.368	0.648	0.002	5.857	3.514	—
	KOCCG-TOP- r	8903	0.849	2	0.007	0.007	0.0	0.056	0.014	0.327	3.417	2.901	—
$k = 4$	LSPCD (AVG)	2288	0.232	4	0.033	0.051	0.869	0.936	0.086	0.23	113.637	26.258	88.288
	LSPCD (STD)	40	0.02	0	0.008	0.005	0.002	0.058	0.001	0.009	2.613	1.623	20.523
	SCG-MA	4852	0.007	4	0.042	0.104	0.82	0.577	0.027	0.241	104.937	0.707	139.274
	SCG-MO	1943	0.056	4	0.063	0.117	0.848	0.533	0.086	0.163	117.935	6.581	69.637
	SCG-B	1700	0.372	4	0.12	0.032	0.768	0.268	0.07	0.174	49.824	18.514	3792.395
	SCG-R	7174	0.048	4	0.006	0.012	0.836	0.308	0.015	0.293	41.125	1.984	131.226
	KOCCG-TOP-1	57	0.085	4	0.708	0.502	0.75	0.891	0.253	0.027	4.456	0.379	—
	KOCCG-TOP- r	4852	0.742	4	0.014	0.011	0.213	-0.075	0.024	0.199	3.821	2.833	—
$k = 6$	LSPCD (AVG)	2394	0.172	6	0.049	0.039	0.873	0.847	0.08	0.233	96.085	16.382	69.593
	LSPCD (STD)	207	0.031	0	0.025	0.007	0.004	0.112	0.006	0.019	4.787	2.244	9.767
	SCG-MA	4827	0.006	6	0.009	0.044	0.821	0.622	0.028	0.243	102.611	0.578	145.295
	SCG-MO	2016	0.037	6	0.06	0.06	0.848	0.685	0.079	0.159	111.578	4.151	76.205
	SCG-B	1924	0.039	6	0.084	0.015	0.771	0.291	0.061	0.174	46.069	1.779	6125.694
	SCG-R	12909	0.128	6	0.011	0.004	0.788	0.135	0.009	0.463	18.278	2.331	175.294
	KOCCG-TOP-1	50	0.074	6	0.765	0.476	0.962	0.633	0.505	0.007	4.904	0.363	—
	KOCCG-TOP- r	4827	0.698	6	0.016	0.009	0.286	-0.209	0.023	0.2	1.522	1.062	—

Table 12: Detailed results on the **Epinions** dataset from various aspects. LSPCD (avg) and LSPCD (std) respectively indicate the mean and standard deviation across five runs of our method with different seeds.

		SIZE	BAL	K	MAC	MAO	CC+	CC-	DENS	ISO	POL	BA-POL	RT
$k = 2$	LSPCD (AVG)	2188	0.44	2	0.12	0.013	0.907	0.74	0.066	0.351	127.784	56.221	59.119
	LSPCD (STD)	4	0.004	0	0.001	0.0	0.002	0.002	0.0	0.0	0.181	0.42	3.692
	SCG-MA	1234	0.02	2	0.088	0.114	0.906	0.739	0.116	0.246	128.316	2.541	34.752
	SCG-MO	1017	0.019	2	0.099	0.138	0.91	0.713	0.14	0.22	128.722	2.446	25.471
	SCG-B	253	0.024	2	0.419	0.205	0.999	1.0	0.621	0.501	156.379	3.768	822.236
	SCG-R	4396	0.091	2	0.01	0.007	0.891	0.766	0.019	0.363	72.282	6.561	12.119
	KOCCG-TOP-1	12	0.4	2	0.708	0.815	1.0	0.833	0.803	0.007	8.167	3.267	—
	KOCCG-TOP- r	1234	0.719	2	0.054	0.022	0.5	-0.245	0.064	0.16	14.036	10.092	—
$k = 4$	LSPCD (AVG)	2120	0.136	4	0.124	0.016	0.932	0.408	0.065	0.341	111.544	14.851	65.489
	LSPCD (STD)	129	0.042	0	0.021	0.003	0.002	0.312	0.004	0.006	7.5	3.548	2.958
	SCG-MA	1576	0.001	3	0.416	0.001	0.928	-0.714	0.09	0.285	127.432	0.107	42.784
	SCG-MO	1373	0.001	3	0.438	0.001	0.934	-0.635	0.103	0.264	128.951	0.129	34.407
	SCG-B	868	0.002	3	0.405	0.0	0.926	-0.411	0.119	0.226	94.43	0.187	2169.558
	SCG-R	1872	0.005	4	0.152	0.033	0.928	-0.801	0.044	0.23	65.124	0.294	49.068
	KOCCG-TOP-1	28	0.455	4	0.865	0.62	0.953	0.582	0.81	0.011	8.905	4.048	—
	KOCCG-TOP- r	1576	0.533	4	0.071	0.01	0.768	-0.63	0.06	0.202	11.001	5.869	—
$k = 6$	LSPCD (AVG)	2660	0.066	6	0.088	0.014	0.929	0.324	0.05	0.373	103.375	6.835	107.579
	LSPCD (STD)	153	0.009	0	0.009	0.004	0.002	0.142	0.004	0.007	3.637	0.857	20.806
	SCG-MA	2564	0.005	6	0.301	0.048	0.935	-0.713	0.05	0.34	88.759	0.448	57.185
	SCG-MO	1373	0.001	3	0.438	0.001	0.934	-0.635	0.103	0.264	129.22	0.129	37.194
	SCG-B	868	0.002	3	0.405	0.0	0.926	-0.411	0.119	0.226	94.476	0.187	3696.279
	SCG-R	1365	0.003	6	0.128	0.036	0.946	-0.898	0.054	0.203	43.324	0.138	53.993
	KOCCG-TOP-1	34	0.444	6	0.9	0.43	1.0	0.496	0.576	0.012	5.965	2.651	—
	KOCCG-TOP- r	2564	0.405	6	0.043	0.006	0.779	-0.654	0.035	0.262	6.802	2.753	—

Table 13: Detailed results on the **WikiPol** dataset from various aspects. LSPCD (avg) and LSPCD (std) respectively indicate the mean and standard deviation across five runs of our method with different seeds.

		SIZE	BAL	K	MAC	MAO	CC+	CC-	DENS	ISO	POL	BA-POL	RT
$k = 2$	LSPCD (AVG)	599	0.151	2	0.093	0.034	0.917	0.87	0.15	0.109	81.985	12.417	57.022
	LSPCD (STD)	2	0.001	0	0.001	0.0	0.003	0.011	0.0	0.0	0.037	0.042	7.851
	SCG-MA	1251	0.007	2	0.035	0.054	0.924	0.928	0.072	0.172	82.822	0.599	11.484
	SCG-MO	648	0.005	2	0.071	0.079	0.928	1.0	0.147	0.121	88.441	0.41	4.041
	SCG-B	609	0.02	2	0.041	0.013	0.963	-0.238	0.081	0.112	46.525	0.932	773.37
	SCG-R	7400	0.082	2	0.003	0.001	0.91	0.63	0.005	0.305	36.119	2.968	76.435
	KOCCG-TOP-1	6	0.6	2	0.75	0.625	1.0	1.0	0.6	0.003	3.0	1.8	—
	KOCCG-TOP- r	1251	0.859	2	0.024	0.012	0.322	-0.284	0.035	0.097	1.258	1.081	—
$k = 4$	LSPCD (AVG)	450	0.075	4	0.147	0.068	0.938	0.546	0.184	0.086	71.628	5.389	83.214
	LSPCD (STD)	23	0.002	0	0.063	0.032	0.002	0.249	0.014	0.003	2.015	0.189	26.749
	SCG-MA	2140	0.013	4	0.093	0.014	0.917	-0.613	0.038	0.217	56.471	0.728	49.769
	SCG-MO	2783	0.0	3	0.283	0.001	0.895	-0.775	0.026	0.242	39.698	0.019	44.39
	SCG-B	727	0.002	2	0.203	0.001	0.967	-0.899	0.07	0.125	45.661	0.076	2225.353
	SCG-R	7740	0.029	4	0.002	0.001	0.916	0.599	0.005	0.302	33.723	0.966	91.037
	KOCCG-TOP-1	26	0.286	4	0.558	0.119	0.949	0.182	0.255	0.005	3.051	0.872	—
	KOCCG-TOP- r	2140	0.27	4	0.02	0.002	0.808	-0.609	0.01	0.092	4.409	1.192	—
$k = 6$	LSPCD (AVG)	825	0.06	6	0.191	0.026	0.94	-0.28	0.093	0.123	58.694	3.532	228.675
	LSPCD (STD)	72	0.001	0	0.023	0.014	0.005	0.183	0.011	0.008	1.548	0.079	192.894
	SCG-MA	2176	0.001	4	0.259	0.001	0.919	-0.73	0.037	0.22	57.546	0.046	54.104
	SCG-MO	2783	0.0	3	0.283	0.001	0.895	-0.775	0.026	0.242	41.846	0.02	48.571
	SCG-B	727	0.002	2	0.203	0.001	0.967	-0.899	0.07	0.125	45.986	0.077	3973.384
	SCG-R	95033	0.002	6	0.006	0.0	0.884	-0.686	0.003	0.901	3.329	0.007	331.066
	KOCCG-TOP-1	83	0.364	6	0.756	0.029	0.967	-0.658	0.268	0.015	10.135	3.685	—
	KOCCG-TOP- r	2176	0.192	6	0.032	0.002	0.867	-0.578	0.006	0.077	3.585	0.687	—